The Pennsylvania State University

The Graduate School

College of Agricultural Sciences

ULTRASONIC CHARACTERIZATION OF CRYSTAL DISPERSIONS

A Thesis in

Food Science

by

Umut Yucel

© 2010 Umut Yucel

Submitted in Partial Fulfillment
of the Requirements
for the Degree of

Master of Science

May 2010

The thesis of Umut Yucel was reviewed and approved* by the following:

John Coupland
Associate Professor of Food Science
Thesis Adviser

Ramaswamy Anantheswaran
Professor of Food Science

John Floros
Professor of Food Science
Head of the Department of Food Science

*Signatures are on file in the Graduate School

ABSTRACT

The aim of this study was to investigate the applicability of ultrasonic techniques to the characterization of crystal dispersions. Longitudinal ultrasonic waves (2.25 MHz) were used to follow the changes in dispersions of sugar crystals (i.e., lactose or sucrose) in different liquid phases (i.e., water or vegetable oil). In general, it was found that the ultrasonic attenuation measurements were more sensitive to the amount and size of the dispersed crystals while velocity measurements were more sensitive to the changes in total concentration (dissolved or undissolved).

Ultrasonic measurements were used to measure the compositions (e.g., concentration) of lactose solutions and aqueous suspensions of lactose crystals. The ultrasonic velocity in lactose-water mixtures (i.e., solution or dispersion) was independent of the state of lactose molecules (i.e., either dissolved or crystallized) and increased almost linearly with lactose concentration. In contrast to the ultrasonic velocity measurements, ultrasonic attenuation was relatively unaffected by changes of lactose concentration in solution, but increased with the amount of dispersed crystals. Similarly in lipid systems, attenuation was low in oil and increased with dispersed sucrose crystal concentration. Furthermore, it was also found in lipid systems that sucrose crystal aggregation (induced by adding water) increased ultrasonic attenuation.

Since ultrasonic attenuation is more sensitive than velocity measurements to the presence of dispersed particles in a liquid, attenuation measurements were used to follow dynamic changes in the dispersed phase through dissolution and crystallization of lactose in aqueous environments.

The dissolution of lactose crystals (d~50 μm) in stirred aqueous solutions was investigated using continuous on-line ultrasonic attenuation measurements and at discrete intervals by off-line refractive index measurements. Upon addition of powdered sugar into water or an under-saturated solution, air pockets between and around the crystal agglomerates strongly attenuated the acoustic signal, and obscured any changes resulting

from the dissolution process until all air was removed. In order to minimize air incorporation, water was added to suspensions of lactose crystals in saturated lactose solution to produce an under-saturated solution and cause crystal dissolution. In this case the rate constant for lactose dissolution evaluated from on-line attenuation measurements (~700 μs^{-1}) was in reasonable agreement with off-line measurements and literature values.

The crystallization of lactose within gelatin gels was also monitored by ultrasonic attenuation measurements using a modified pulse-echo reflectometer as an immersion probe, and results were compared to turbidity and isothermal differential scanning calorimetry measurements. The gel environment prevented crystal sedimentation and hindered convection flow effects and secondary nucleation. The crystallization rate of lactose was increased with increasing degree of supersaturation, but relatively unaffected by gelatin concentration. The kinetic parameters for growth rate and induction time varied in a similar way with changes in lactose and gelatin concentration for all methods. Although it is difficult to make conclusions about the relative effects of gelatin-lactose interactions on lactose crystallization, ultrasonic measurements were able to differentiate between different crystallization conditions.

Finally, the effects of dispersed crystal (de)aggregation on ultrasonic attenuation were studied using the model of sucrose crystals dispersed in oil (8-16 wt%). During the dispersing process, powder agglomerates are broken up and the viscosity of the suspension decreases (e.g., chocolate conching). It was found that the deagglomeration of sucrose crystals (i.e., dispersing the sugars in a liquid uniformly) in oil was much slower than in an aqueous environment due to the hydrophobic nature of the oil and the possible presence of small amounts of water at the crystal surfaces. Attenuation increased linearly with concentration, and also with increasing effective particle size. Additionally, when crystal aggregation was triggered by the addition of small amounts of water (≤1 %), the ultrasonic noise also increased, which may be due to either uneven distribution of agglomerates or the inhomogenity of the agglomeration process (i.e., diverse particle size distribution and morphology). Finally, the stirrer was switched off and the crystals and

aggregated crystals were allowed to sediment out of suspension. The subsequent sedimentation kinetics, as followed at a certain height from the bottom of the container through the ultrasonic beam path, was used to provide further information about the state of agglomerated sucrose crystals. It was found that the addition of 1% (vol. water/wt. sucrose) decreased the total sedimentation time to half that of the water-free samples. In addition, the agglomeration process was shown to be inhomogeneous yielding uneven sedimentation profiles, as the degree of inhomogeneity was confirmed by micrometer measurements.

TABLE OF CONTENTS

LIST OF TABLES

LIST OF FIGURES

ACKNOWLEDGEMENTS

Completion of this thesis could not be accomplished without many people's contributions, help and encouragement. I would like to mention those who deserve my sincere acknowledgement.

First of all, I would like to express my sincere gratitude to my supervisor Dr. John N. Coupland for being not only a prosperous guide in my academic career, but additionally a great mentor. His deep patience and valuable time ensured the completion of this work. I learnt much from him, but there is still a big deal more to learn.

I would like to thank my committee members, Dr. Ramaswamy Anantheswaran and Dr. John D. Floros for their valuable time as well as invaluable help and encouragement.

I would like to thank former and present lab-mates for their help and support, or at least just being there when needed. My special thanks are for Dr. Ibrahim Gulseren and Dr. Ying Wang for their great help and support in my first years in Penn State. I would also like to thank all Food Science Department family for creating this positive atmosphere and making my graduate life a here better one. I would like to thank all my friends in State College for their precious help whenever I need it, and making State College bigger place than as it seems. I would like to give my special thanks to my flat-mate, Cem Topbasi for his invaluable and everlasting help and great company. I must extent my heartiest thanks to my friends back in Turkey for their most valuable support and being next to me even there is an ocean in between.

I would like to thank Dr. Valentina Trinetta for her support, patience and heartiest company.

I would like to give my special thanks and love to my family in Ankara, Turkey. As in all parts of my life, without their support this work could not be accomplished.

Chapter 1

INTRODUCTION AND LITERATURE REVIEW

1.1. Crystals in foods

1.1.1. Introduction

Many foods are dispersions of crystals in a liquid phase. The crystalline structure, which can change during manufacturing or storage, determines the texture, sensory attributes, and stability of the product. The formation of crystals within the continuous phase can be desirable (e.g., fat fractionation, sucrose refining, small ice crystals in ice cream) or undesirable (e.g., sucrose crystals in hard candy, lactose crystals in ice cream). Crystals can be formed either from bulk solution (e.g., ice formation in ice cream manufacturing) or dispersions of seed crystals (e.g., cocoa butter in chocolate tempering process) which provides more control over the crystal characteristics. In either case, an effective process and formulation control is essential to optimize product quality.

1.1.2. Theory of crystallization

Thermodynamics

A solution is a homogenous mixture of dissolved solute molecules in a continuous liquid phase (i.e., solvent). The distribution of solute molecules within the solvent is defined by the balance of enthalpic and entropic terms, yielding a condition to minimize the Gibbs free energy of the system.

Beyond a specific concentration (i.e., solubility limit), solute molecules at equilibrium do not distribute themselves homogenously but instead form a separate phase. The solubility limit is a function of temperature, as well as formulation determining the phase behavior of the components in the system. The solubility limit of solids in liquids decreases with temperature. If a solution is cooled, the solubility limit can go lower than the

concentration of the dissolved solute molecules, yielding a super-saturated solution. Thus, the thermodynamic driving force due to the excess free energy in the system may drive the solute particles to crystallize out, a specific case of phase separation.

Crystallization, in general, proceeds via two distinct processes: crystal nucleation and growth (Garside, 1985), rate of which determined by the extent of driving force (i.e., degree of super-saturation), but limited by kinetic constraints. There are also additional processes, such as Ostwald ripening or crystal perfection, leading the crystalline structure to a lower energy state without further changing the total amount of crystals.

Kinetics

i. Crystal nucleation

Nucleation is the phase separation process leading to the formation of the crystal nuclei. There are two main groups of nucleation mechanisms, primary and secondary (Fig. 1). In primary, or spontaneous, nucleation, solute molecules first form molecular clusters, crystal embryos. Only crystal embryos larger than a critical size (proportional to the logarithm of the degree of supersaturation) are stable and will begin to grow to form macroscopic crystals (Garside, 1985). In homogeneous nucleation, the formation of crystal embryos is merely determined by molecular kinetics of solute and in most practical circumstances is too slow a process to be relevant. In practice, there are often impurities in the solution, such as dust particles or imperfections at the boundaries, that may serve as attachment sites for solute molecules, and thus aiding nucleation by lowering the free energy change required (i.e., heterogeneous nucleation) (Myerson and Ginde, 2001).

Secondary nucleation is defined as “nucleation which takes place only because of the prior existence of crystals of the material being crystallized” (Botsaris, 1976). Garside (1985) classified it as apparent, true, and contact secondary nucleation. Apparent, or initial, secondary nucleation is due to the fragmentation of the dry crystals when they are first introduced to the super-saturated solution. The true secondary nucleation occurs when the super-saturated solution is metastable (i.e., it does not crystallize readily), and

the addition of subcritical size nuclei disturb the steady state condition and allow crystal growth. Contact, or collision, secondary nucleation is the most abundant among three, and occurs due to the fragmentation of growing solute crystals by contacts/collisions with each other and other surfaces such as, container walls or impeller (Garside, 1985). Contact secondary nucleation is an important mechanism in industrial processes such as refining of sugars or fractionation of fats (Hartel, 2001).

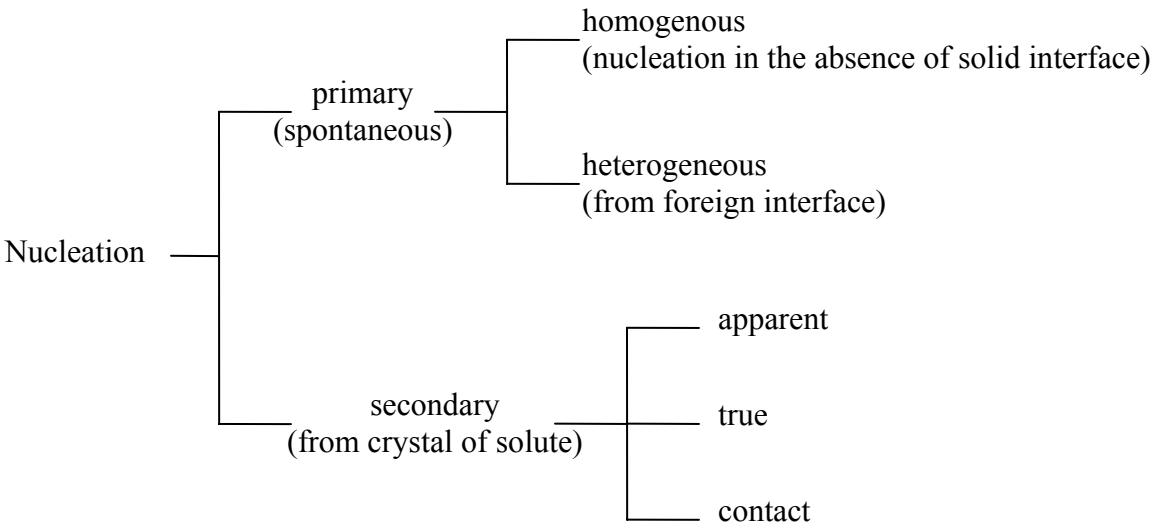

Figure 1.1. Nucleation mechanisms (adapted from Garside, 1985).

Nucleation kinetics, especially primary nucleation, can be investigated by two correlated phenomena: the rate of nuclei formation (i.e., number of stable nuclei formed per unit volume per unit time), and time required for nucleation to occur (i.e., the induction time). In practice, the measured induction time is off-set by the sensitivity of the detector, thus quantification of the real nucleation rate is difficult.

ii. Metastable zone

When a solution is supersaturated (i.e., the concentration is greater than the thermodynamic solubility) excess free energy forces the dissolved molecules to phase separate. However, while the free energy change for forming large crystals is negative

and thus occurs spontaneously, the free energy change to form a small crystal is positive and can provide a kinetic barrier to crystallization.

If the rate of formation of stable crystal is too slow to be observed in a practical time scale, the system is defined as metastable. Furthermore, since crystallization requires diffusion, conformation change and surface incorporation of solute molecules, as well as the removal of latent heat of crystallization, factors affecting these processes can hinder or catalyze the nucleation event. Thus, the metastability of a system is generally determined by the characteristic of the system (e.g., dynamic of the solute molecules, or viscosity of the solution) and the history of the solution (e.g., cooling rate, concentration of impurities, or degree of mixing). However, with exceptionally high cooling rates, molecular mobility of the molecules would be hindered, resulting in very long induction times, and may result in solid-like samples (i.e., glass-transition).

The metastable zone (width) can be defined as the concentration range at a defined temperature between the solubility limit and concentration at which nucleation occurs spontaneously upon further increasing the degree of supersaturation (Hartel, 2001). Moreover, metastable zone width can further be defined with respect to type of nucleation, where it is largest for the primary nucleation (Ulrich and Strege, 2002). The metastable zone can be minimized to a "false-grain zone" by introducing solute crystals under shear, i.e., secondary nucleation (Hartel, 2001). Knowledge of the metastable zone is required to adjust operation parameters as desired in an industrial crystallization processes. For example, according to Omar and Ulrich (1999) the optimum degree of supersaturation promoting the crystal growth over nucleation is approximately half width (i.e., mean concentration between the limits defining the metastable zone) of the metastable zone.

iii. Crystal growth

After stable nuclei are formed, they grow larger by addition of solute molecules, which in turn decreases the total free energy of the crystal, as long as the solution is super-saturated and the molecules have enough mobility. Three primary mechanisms are

important in controlling the rate of crystal growth: mass transfer processes, surface incorporation, and heat transfer effects (Hartel, 2001). The growth rate of a crystal plane (i.e., face) can be different than the others as determined by the surface free energy change on that plane and results in a characteristic shape for the macroscopic crystal.

The reverse process, dissolution, is the opposite of crystal growth but as it does not require a nucleation event the rate is only affected by changes in heat/mass transfer at the crystal surface (Ulrich, 2003).

Although crystal nucleation and growth are separate processes, they can occur simultaneously. The relative rates of crystal nucleation and growth determine the number and size of the crystals (i.e., crystal size distribution, CSD). Generally, by increasing the degree of super-saturation (or super-cooling) the nucleation event is promoted over crystal growth, yielding a larger number of smaller crystals. Alternatively, crystallization from solution by using crystal growth templates (i.e., seeded crystallization) allows more control over crystalline structure, since nucleation event can be restricted to secondary nucleation by carefully controlling the degree of super-saturation. On the other hand, there are several other factors that can affect CSD, such as the presence of impurities in the system, imperfections at the boundaries, degree of the applied shear, and heat and mass transfer phenomena in the system.

Crystals of similar size and shape in the same environment may grow at different rates (i.e., growth rate distribution). Although the mechanism is not fully understood, it has been attributed to the secondary nucleation events (Ulrich, 2003), or to dislocations and presence of impurities on the surface and the crystal history of the microstructure (Hartel, 2001).

1.1.3. Properties and characterization of crystal dispersions

In general, crystal dispersions can be characterized in terms of the crystal concentration, size distribution, morphology and micro-structure, as well as the change of these

parameters with time. Measurement of bulk properties, such as texture or rheology, of the system can be used as a quality control tool, and can be related to crystalline structure and composition. However complete characterization of the system requires combinations of different techniques, such as microscopy (i.e., optical microscopy or electron microscopy), optical techniques (i.e., light scattering within the suspension and optical rotation or refractive index of solution), nuclear magnetic resonance (NMR), x-ray diffraction (XRD), or thermal analysis (i.e., differential scanning calorimetry, DSC), each sensitive to different attribute of the crystal dispersion. There is still need for alternatives, since every technique has its characteristic limitations and drawbacks.

Crystal microstructure

A crystal is defined as a solid structure built from atoms or molecules forming a periodic repeating pattern in three dimensions (Myerson and Ginde, 2001). The crystal structures are classified by means of "space lattice" (or point lattice) showing the location of atoms or molecules by using three spatial dimensions and angles (i.e., Miller indices). The unit cell defines the shape of the periodic parallel-sided structure of lattice points. There are 14 possible point lattices (i.e., the Bravais lattices) that atoms or molecules are packed into crystals (Brandon and Kaplan, 2008). Each crystalline material has its characteristic lattice structure and parameters, consequently resulting in varying bulk properties. Moreover, phase equilibria and crystal growth conditions can cause different lattice structures (i.e., polymorphs) for certain atoms (e.g., graphite and diamond polymorphs of carbon) or molecules (e.g., cocoa butter shows 6 different polymorphs, type I-VI).

The fundamental method to determine the crystal microstructure is the XRD spectroscopy. Depending on the spacing of crystal planes (i.e., lattice parameters), x-rays will be diffracted in a specific angle and wavelength dependent manner (i.e., Bragg's Law). Each crystalline material has its unique XRD pattern. Although there are many XRD based measurement techniques, powder XRD is one of the basic and commonly used techniques to characterize crystalline microstructure in food materials, providing the material can be formed into micron-size randomly distributed crystal powders. X-ray techniques typically require such long measurement times during which product should

not change its properties. However, XRD measured using synchrotron radiation (i.e., high energy x-rays) allows more rapid analysis (i.e., within seconds).

DSC in temperature scanning mode can provide indirect information about the crystal microstructure, as well as the concentration. When the molecules crystallize, latent heat is released and can be calculated from the DSC curve as an exothermic peak. The opposite is true for melting where an endothermic peak is observed. Each crystal polymorph has a characteristic crystallization (or melting) temperature and enthalpy. The area under the crystallization curve can be used to measure the enthalpy of the process, and together with phase transition temperature information, the crystalline structure can be inferred. The sensitivity of this indirect measurement technique relies on the scan rate, which affects peak resolution and position. DSC and XRD techniques are often used to complement one another which can be particularly useful for materials showing complex polymorphic transitions such as lipids (Higami et al., 2003).

Concentration

There are many methods used for monitoring crystal concentration. Some of them require separation of crystals from the solution (e.g., sedimentation or sieving) and analyzing separately, while there are other techniques used directly on the crystal and solvent mixture (e.g., NMR, XRD, DSC, or turbidity).

The solid fat content of fatty products is widely determined by NMR spectroscopy. This technique is based on the absorption of radio frequency electromagnetic radiation by a certain nuclei aligned in a magnetic field. The structure and environment of the molecule, thus the crystal concentration, can be inferred from nuclear relaxation time measurements. However, NMR methods are often relatively slow and expensive and cannot make measurements inside metal containers. A related technique, electron paramagnetic resonance (EPR), relies on the absorption of electromagnetic radiation (i.e., microwaves) by unpaired electron(s), however this methods limited to the presence of EPR active molecules (i.e., free radicals). Gillies et al. (2006) used this technique to study the changes in ice cream during freezing and melting.

The degree of crystallinity can also be measured from a DSC thermogram as areas of the phase transformation peaks of different crystalline structures. However, this technique is more suitable for simple model systems, since other thermodynamic changes such as gelatinization, chemical reactions, or moisture loss may affect the peak properties. Moreover, construction of a realistic baseline is essential to analyze the thermogram appropriately.

In a similar manner, the areas of diffraction peaks obtained from the XRD spectroscopy can also be used to measure the concentration of crystals. However, low crystal concentrations may be difficult to monitor since the diffraction pattern can be masked by diffuse background diffraction, unless a high energy source radiation is used (i.e., synchrotron radiation). In addition, there are various factors in powder XRD technique that can lead to discrepancies in the analyses. Since the XRD patterns of crystalline materials result from the elastically scattered x-rays by electrons, the peak shape and intensity is, in general, can be determined by utilizing scattering theories. Other than the experimental factors such as surface roughness and displacement, artifacts of the system include polarization factor (i.e., dependence of intensity to scattering angle, 2θ), structure factor (i.e., defined by the lattice parameters), multiplicity factor (i.e., number of reflections from crystal planes of the same family), Lorentz factor (i.e., geometric factors), absorption, and temperature factor.

A simple way to measure total crystal concentration is through turbidity measurements provided that the crystals are uniformly dispersed and system remains optically transparent. This technique can be used on-line. However there are limitations, common to other optical methods, and quantification of the total crystal concentration can be unrealistic (Marangoni, 1998). Firstly at higher concentrations the dispersion can become optically opaque. Secondly, turbidity is not always directly proportional to concentration due to multiple scattering and particle size effects. Finally, there may also be additional intensity losses due to absorption within the particle, which can be a particular problem for particles larger than $\lambda/20$, where λ is the wavelength, and also to refraction of the incident light, which is especially important for birefringent materials.

In addition to the amount of crystals, their size and morphology are needed to be controlled for an optimized product and process. Knowing the number of crystals present and their size distribution, crystal concentration can also be calculated.

Size distribution

There are many techniques available for crystalline-particle sizing, each with characteristic pros and cons, and suitable for specific systems and processes. The first group of methods relies on mechanical separation principles and varies from simple sieving to chromatography-like systems as in field flow fractionators. In simple sieving the crystals are passed through a number of sieves with different mesh sizes, and the amount retained in each size category can be used to calculate the histogram of crystal size distribution. Prior to sieving, crystals can be separated from solution either by simple filtration or sedimentation. The principle of sedimentation devices considers the Stokes radius of the particles and density difference of the particles and the liquid phase to separate them in an external force field (i.e., centrifugal or gravimetric). Another separation technique is electrical sensing zone method (e.g., Coulter Counter apparatus), which determines the CSD in an electrolyte solution. In this technique, the electrical impedance change is measured as particles pass through a small orifice, which in turn displace their own volume of electrolyte. However, these methods are often not suitable for crystals dispersed in food products, since they might be embedded in a complex environment (e.g., ice cream), and not readily separable from the bulk.

Optical techniques (i.e., light scattering methods) are the second group of methods to measure CSD. These methods are fast, sensitive, and nondestructive, but are still subject to the constraints common for optical methods. Two groups of light scattering techniques are commonly used: static light scattering and dynamic light scattering (photon correlation spectroscopy, PCS) (Karpinski and Wey, 2001). A wide range of particle sizes from submicron (i.e., from 0.1 μm) up to millimeter scale (i.e., 1-2 mm) can be determined effectively by static light scattering method, which is based on the dependency of the diffraction angle on the particle radius (Fraunhofer spectra). On the other hand, PCS measures the changes in the intensity of the scattered light due random

Brownian motion of the dispersed particles in the sufficiently transparent continuous liquid phase. This method is sensitive to smaller particle sizes from couple of nanometers to about 3 μm. In a similar manner, small angle x-ray scattering (SAXS) or small angle neutron scattering (SANS) can be used to determine CSD of nano-scale particle dispersions. Both static and dynamic light scattering methods are not direct measurements of CSD, but rather use light scattering effects with spherical particle approximation.

Finally, optical and electron microscopies coupled with image analyzing protocols can quantify the CSD. However, this approach requires large number of images analyzed collectively in order to give realistic and statistically valid results. The morphology of the crystals, as well as their size, can also be analyzed by microscopy.

Shape and aggreagtion

Crystal habit (i.e., morphology of the crystals) is both influenced by the intrinsic factors of the molecular crystal and external growth conditions. The shape of the crystals is determined by the relative area of faces formed (i.e., relative growth rates of individual faces) and is characteristic of the particular formulation, as well as the crystallization conditions. For example, when lactose crystals were obtained by crystallization from bulk aqueous solution, with fast crystallization rates, only prisms are formed. However, with decreasing degree of super-saturation diamond shaped plates, then pyramids and tomahawk shape were observed (Herrington, 1934). Moreover, the presence of impurities (i.e., acting as either growth inhibitors or actuators) can also affect the crystal morphology. Hunziker and Nissen (1927) showed that α-lactose monohydrate crystals obtained from aqueous solutions have their characteristic “tomahawk shape”, whereas if the solution contains high concentrations of sucrose, the shape of the lactose crystals were “short, truncated pyramids with flat rhomboid base and apex”.

Over time the CSD and shape can change, as larger crystals grow at the expense of smaller ones via a process known as Ostwald ripening. Moreover, upon storage, crystals may change their polymorphic form or aggregate, provided that the molecular mobility or

colloidal mobility is not hindered. In any case, free energy of the crystals will be lowered as the total amount of crystals remains unchanged. Aggregated crystals can form a network which will affect the rheological properties of the dispersion. It is generally expected that the apparent viscosity of the dispersion to increase with degree of agglomeration. Particle sizing techniques, as well as microscopy, can be used to follow the aggregation phenomenon.

Monitoring the kinetics of crystal growth and nucleation

Since rates of crystal growth and nucleation affect the properties of crystal dispersion and consequently the quality and stability of the final food product, it is essential to know and control the kinetics of change. Although crystal nucleation and growth are separate events, they can occur simultaneously and affect each other. Consequently, monitoring and evaluating them individually can be challenging and may require combination of different techniques.

Techniques sensitive to concentration can further be utilized to follow mass crystallization kinetics or just the presence of crystals (i.e., induction time). While the overall rate of mass crystallization can be calculated from the rate of change of sensor response, the induction time can be inferred from the lag time for significant deviation from the initial response. Wright et al. (2000) compared different methods used in lipid crystallization studies, and concluded that the response of different techniques can be similar in trend but varying in sensitivity. Moreover, the complexity of the crystalline system, usually the case for foods, negatively affects the sensitivity and resolution of the used technique. For example, the presence of crystals, thus the induction time might be investigated by XRD, however the diffuse background will decrease the sensitivity; such that 5 to 10 % of crystalline material is required in a sugar glass to distinguish XRD pattern from the background (Hartel, 2001). Such a large lag time makes this technique unsuitable for nucleation kinetics study. XRD technique can be utilized to evaluate the total crystallization kinetics, but there are still several factors (from sample surface height and roughness to precise temperature control) causing the potential for significant error.

On the other hand, if the system has enough transparency in the beginning, the induction time can be evaluated in a precise manner using optical methods, such as turbidity. DSC in isothermal scan mode can also be used to study crystallization kinetics. In this technique, a solution is quickly cooled to a super-saturated state and the temperature is kept constant at that crystallization temperature. The rate of change of crystallinity can be monitored from the change of area of the exothermic peak with time. This method is associated with a lag time where the system takes a finite time to cool to the starting temperature. If the rate of crystallization is rapid enough, so the short induction time could be in the non-isothermal period, resulting in overestimation of the induction time.

As the crystallization kinetics can be monitored directly by following the CSD (i.e., increase in crystal size) over time, it may also be followed indirectly by monitoring the changes in the solution properties, such as density, refractive index, and optical rotation measurements. Density of the solution will change approximately linearly with the concentration of dissolved solute. Refractive index and optical rotation measurements are commonly used in sugar and dairy industries. The theory of refractive index measurements uses the fact that light can be refracted when the media is changed, obeying the Snell's Law. Refractive index of a solution, as measured by a refractometer, is a measure of degree of refraction depending on the speed of light in the solution, which is a function of amount of dissolved solute, relative to air. Optical rotation measurements can be used as another optical method to measure the concentrations of solutions of optically active materials (i.e., having circular birefringence). When polarized light passes through an optically active material, the plane of polarization is rotated. This rotation can be measured by a polarimeter, and the concentration can be calculated from the specific optical rotation of solution, the angle by which the plane is rotated per unit concentration and per unit length (Walstra and Jenness, 1984). The specific optical rotation not only depends on material but also is different for different stereoisomers (e.g., at 20°C for α- and β-lactose in water are +89.4° and +35°, respectively, and +55.3° for the equilibrium mixture) (Holsinger, 1997). Combination of independent measurements of solution properties and CSD may enable to achieve separate crystal

nucleation and growth information, together with more accurate and realistic nucleation kinetics.

Aside from nucleation, growth or dissolution, kinetic changes in crystal dispersions can also be due to (de)aggregation of the crystals. For example, in conching step of chocolate manufacturing, non fat solids (i.e., sugar) and milk powder (containing lactose molecules) in the case of milk chocolate is uniformly dispersed in cocoa butter and the degree of agglomeration can be followed indirectly by the amount of energy required to mix the suspension at a constant speed (Beckett, 2001). A similar process is involved in the preparation of flavor slurries (i.e., dispersions of sugars, salts and flavors in oil) whose quality may be affected by distribution and agglomeration of the crystals.

Need for alternative and on-line methods to follow crystallization

All available techniques have their characteristic limitations, and none is readily applied as an on-line monitoring tool to characterize crystal dispersions. Utilizing alternative techniques can provide more thorough information. Ultrasound based methods are fast, inexpensive, noninvasive and can be applied as on-line tools to monitor changes in crystalline properties of optically opaque systems.

1.2. Ultrasound

1.2.1. Properties of the acoustic wave

Sound is a mechanical wave travelling through a media as spatially and temporally varying pressure. The specific type of sound propagation where the molecular displacements (oscillations) are parallel to the direction of wave propagation is called a longitudinal (or compressional) wave. The simplest way to define an acoustic wave in the fluid media is by the linear acoustic wave equation (Kinsler et al., 2000):

$$\nabla^2 p = \frac{1}{c^2}\frac{\partial^2 p}{\partial t^2} \qquad (1.1)$$

where p is the acoustic pressure fluctuation, ∇^2 is the Laplacian operator, t is time, and c is the thermodynamic speed of sound (defined as $c = \sqrt{\frac{B}{\rho_0}} = \lambda f$, where B is the bulk modulus and ρ_0 is the equilibrium density of the system, f is ultrasonic frequency (Hz) and λ is wavelength). A simplified general solution can be obtained by assuming a harmonic plane wave propagating in one direction in a lossless medium (Kinsler et al., 2000):

$$p(x,t) = Ae^{j(\omega t - kx)} + Be^{j(\omega t + kx)} \qquad (1.2)$$

where A and B are constants (i.e., showing the peak magnitude during wave oscillation), ω is the angular frequency (=2πf), j =√-1, k is the wave-number (or propagation constant, k = ω / c = 2π / λ), x is the position of the wave (i.e., the distance it travelled), and the quantity (ωt – kx) is the phase of the wave.

The magnitude of pressure fluctuations determines the energy (intensity) of the acoustic wave, so the degree of molecular movement (i.e., deformation) in the media that they pass through. Thus, the acoustic intensity (I) can be defined as a product of effective pressure amplitude (i.e., acoustic pressure amplitude divided by √2) and effective fluid velocity (i.e., fluid velocity divided by √2), or in a simpler way:

$$I = \frac{1}{2}\frac{P^2}{\rho_0 c} \qquad (1.3)$$

where P is the acoustic pressure amplitude. The intensity of a sound wave (Equation 1.3) is conventionally given in decibel (dB) scale, which is an arbitrary unit defined with respect to a reference value, i.e. for water and other liquids 6.76×10^{-19} W/m^2 (Kinsler et al., 2000).

$$\text{Sound Intensity Level} = \text{IL} = 10\log\left(\frac{I}{I_{ref}}\right) \qquad (1.4)$$

High frequency sound waves, i.e. above the range of human hearing (>18 kHz), are called ultrasound. If the molecular displacement is within the elastic limit of the bonds, as is usually the case with low intensity ultrasound, then the technique is nondestructive and useful for sensing applications (Povey, 1997; Coupland, 2004).

1.2.2. Acoustic propagation in homogenous bulk fluids

The capacity of a material to transmit sound can be characterized in terms of ultrasonic velocity and attenuation. Velocity is typically measured as the time for a sound to travel a known distance and attenuation as the loss of energy, i.e., reduction in sound intensity level per unit distance, as the wave propagates. Equations 1.1 and 1.2 are valid when there is no attenuation within the system, whereas the properties of a longitudinal wave are related to the physical properties of an attenuating media as:

$$\frac{\omega}{k} = \sqrt{\frac{M(\omega)}{\rho}} \qquad (1.5)$$

where ω is the angular frequency, k is the complex propagation coefficient (= ω / c + jα, where c is ultrasonic velocity, α is the attenuation coefficient), ρ is the density and M is the complex elastic modulus of the material supporting the sound wave. Density and modulus are readily related to changes in composition and structure which provides the physical basis for the use of ultrasound as a sensor (Povey, 1997).

Reduction in sound intensity level, i.e., attenuation, can be evaluated as the difference in sound intensity level (Equation 1.4) between two points where the wave propagates and can also be given in dB scale. However the attenuation coefficient, which can be defined

as the reduction in sound intensity level per unit thickness, is conventionally given in nepers per meter, Np/m, which is equal to the 1/8.686 dB/m:

$$\alpha = \frac{1}{d} 10 \log\left(\frac{I_0}{I_1}\right) \qquad (1.6)$$

where α is the attenuation coefficient in dB/m, and I_0 and I_1 are the intensities of sound at two points between which the wave travelled a distance, d.

Attenuation is a term describing the total energy loss as a result of different mechanisms. In a homogenous, one-phase media attenuation results from different mechanisms: absorption through viscous and thermal conduction effects, as well as molecular (or chemical) relaxation in bulk fluids. Absorption is a process that converts acoustic energy into heat energy which can no longer be used to generate sound. In complex fluids where one material is suspended in a second, the situation becomes more complex as the particles can scatter sound in a frequency-dependent manner.

1.2.3. Acoustic propagation in heterogeneous fluid media

Although many mechanisms can contribute to attenuation, the most important in a heterogeneous media are scattering losses. When an acoustic wave encounters a suspended particle dispersed in a continuum, it changes its properties (i.e., scattering) in a frequency dependent manner. Scattering is a re-directivity process, accompanied by associated viscous and thermal scattering-related losses. The particle itself may behave like another acoustic source when interacting with a propagating wave and create wave profiles different than the original. The observed acoustic field is therefore the sum of the unmodified portion of the incoming wave and outgoing wave produced by the particle. Although this redirectivity process, *per se*, does not result in energy loss in total, there are two important scattering mechanisms converting the acoustic energy to heat, visco-inertial scattering and thermal scattering. Consequently, attenuation coefficient of a heterogeneous system is mostly determined by the extent of scattering events. Moreover,

scattering can also change ultrasonic velocity. The sum of the original (unscattered) and scattered waves may posses a different phase than the original resulting in a different phase velocity, which can be detected by a phase sensitive transducer.

The density difference between the dispersed particles and continuous phase is responsible for viscoinertial scattering. The oscillating contractions and rarefactions move particles with respect to the fluid element they are dispersed within due to the density differences. This particle movement results in a drag force around the particle surface, which in turn converts the acoustic energy to heat. Although this effect increases with density contrast, increase in inertia (i.e., viscosity of the continuous phase) will reduce the viscous scattering.

In addition, an ultrasonic pressure wave is associated with a thermal wave fluctuating with amplitudes of few millikelvins. Consequently, there will be heat flow between cold (rarefied) and hot (compressed) regions. This small energy change due to heat flow can be important for systems composed of small density contrast materials, for which the viscous mechanism is hindered.

Sound propagation in heterogeneous media depends on the size and concentration of the dispersed particles, the differences between the thermal and physical properties of two materials, and also the wave-number of the sound. As scattering losses carry valuable information about the dispersed particles, several scattering models were developed to predict ultrasonic properties of dispersions from composition and particle size distribution information, or vice versa (Challis et al., 2005).

All the models have limitations determined by the assumptions made in their development. These assumptions are summarized in detail elsewhere (see Povey, 1997). Assumptions related with dispersion properties, such as size and volume fraction of the dispersed particles, or thermal and physical properties of the respective phases, limits the applicability of the model to certain systems. Although many different models can be found in the literature (see Challis et al., 2005), two broad approaches were followed for

the theoretical formulation of sound-particle interactions: simultaneous solutions to linearized equations (i.e., equation of continuity, conservation of momentum, and equation of state) in derivations or coupled-phase approach. In either case, it is essential to specify the size of the scattering particles relative to the wavelength of the sound. Different models are of concern depending on whether the particles at the long wavelength limit ($kr < 1$, where k is the wave number and r is the radius of the suspended particle) or not. For example, systems of 2.25 MHz ultrasound and particles with diameters up to 100 μm dispersed in aqueous environment can be considered in the long wavelength limit.

The Urick equation is the simplest model, and predicts the solid content of a dispersion from ultrasound velocity measurements using the difference in adiabatic compressibility of solid and liquid phases (Povey, 1997). For a n-component system, the general from of the equation is:

$$\frac{1}{c^2} = \left(\sum_{i=1}^{n} \frac{\phi_i}{c_i^2 \rho_i} \right) \left(\sum_{i=1}^{n} \phi_i \rho_i \right) \qquad (1.7)$$

where φ_i, c_i, and ρ_i are the volume fraction, ultrasonic velocity, and the density of the i^{th} component, respectively, and c is the measured speed of sound in the bulk system. This equation can be simplified by assuming equal densities for the phases present, and for a two component system is:

$$\phi = \frac{1/c^2 - 1/c_l^2}{1/c_s^2 - 1/c_l^2} \qquad (1.8)$$

where φ is the volume fraction of the dispersed particles, c, c_l, and c_s are the speed of sound in the dispersion, liquid phase itself, and solid particles, respectively. Although this model is regarded as a scattering model, the velocity is considered as independent of sound frequency, and viscous scattering and thermal processes are not considered. Thus,

it is only applicable to very dilute systems with very small particles (i.e., long wavelength limit assumption) compared to the wavelength, i.e., very weak scatterers.

The microscopic model of Epstein-Carhart (1953) and Allegra-Hawley (1972), known as ECAH theory, is regarded as the gold standard as for dilute systems of monodisperse and spherical particles in the long wavelength limit, as it considers both thermal and visco-inertial effects (Tebbutt and Challis, 1996). In addition, multiple scattering events can also be considered by modifying the series solutions of the wave number equations in ECAH theory (Waterman and Truell (1961) and Lloyd and Berry (1967). It has been shown that the ECAH theory agreed with experiments for a wide range of conditions. As For example, the ultrasonic properties of a variety of mono-dispersed colloidal systems with a range of density contrast between the dispersed and continuous phases, particle concentration (5-45%), and particle diameter (200-615 nm), were measured as a function of frequency (2-55 MHz), and consequently ECAH theory was utilized as the basis for a particle sizing technique (Holmes et al., 1993, 1994).

The coupled-phase models (e.g., Harker and Temple, 1988) are the second approach to evaluate the sound propagation through dispersions. These models consider each phase separately and are based on visco-inertial coupling of phases (i.e., drag force of one phase acting on the other). Particle shape effects and wide concentration ranges can be considered in these models, but still only in the long-wavelength limit. The most useful advantage of coupled phase models is that they require fewer physical and thermal properties of the components of the system. However, they do not consider thermal losses, so are limited to systems with high density contrast.

Dispersions considered in the food industry can be a mixture of small and large particles with irregular shapes. There is still no complete general model describing acoustic propagation through dispersions of large particles (i.e., outside the long wavelength limit), where geometrical scattering is of concern. Faran (1951) developed a model relating the frequency and particle size to density and elastic properties of the components of the system in the intermediate wave regime (i.e., $kr \approx 1$). This model

utilized the elastic scattering events (i.e., diffraction, refraction, and reflection) as the dominant scattering mechanism and neglected the visco-inertial and thermal scattering effects, making the model unsuitable for particles in the long wavelength limit where these effects dominate. Hay and Mercer (1985) expanded the Faran approach by including the visco-inertial effect by following a similar approach as in ECAH theory, and thus this model is a candidate to characterize the complete range of particle sizes. However, it still lacks the effects of thermal processes and has not been experimentally validated. An example of the use of a mechanistic model in the large particle size limit is provided by Richter et al. (2005, 2006). Modified Faran theory was used in combination with ultrasonic attenuation spectroscopy (3-99 MHz), for size measurement in homogenous particles and emulsions (i.e., with diverse acoustic contrast), as well as porous (i.e., non-homogenous) particles in the micrometer range, but at very low concentrations (i.e., 1%).

All these particle sizing approaches consider the dispersions in the absence of phase change. The phase transition process itself, other than the changes in physical and thermal properties of the system, can affect acoustic propagation and cause deviation from scattering theories. Since pressure fluctuations are associated with temperature fluctuations, the interactions of ultrasonic waves with crystallizing molecules may be sufficient to disturb the instantaneous equilibrium as a frequency dependent manner (Akulichev and Bulanov, 1981, 1983), and absorb ultrasonic energy. If the relaxation time of the molecules undergoing phase change process equals the period of the sound wave, then the ultrasonic absorption will be maximum (Blitz, 1967). This effect has been observed by McClements et al. (1993) who noted that melting transitions in emulsion droplets can cause changes in ultrasonic attenuation and velocity measurements. More recently, an excess ultrasonic attenuation as a result of same phenomenon was observed by Gulseren and Coupland (2007) during the melting of octadecane in water emulsions.

1.3. Ultrasonic characterization of crystal dispersions

There are two general approaches to the characterization of crystal dispersions by ultrasound: spectroscopic analysis of crystal size and concentration within the dispersion using scattering theories, or measuring the macroscopic properties of the system and empirically relating them to crystal properties.

Ultrasonic spectroscopy has been used successfully for particle sizing of well-defined systems in the long wavelength limit, such as emulsions, by means of idealized scattering theories, and to a less extent for dispersions of large size crystals. There have been efforts to follow crystallization by ultrasonic techniques, and corresponding CSD change simultaneously using ECAH theory. For example, the change in the CSD during crystallization of copper (II) sulphate pentahydrate from bulk (Tebbutt et al., 1999) and seeded (Marshall et al., 2002) solutions were calculated from ultrasonic spectra using ECAH theory. However, the results showed some deviation from light scattering measurements. In a similar process, ultrasonic attenuation spectroscopy (2-160 MHz) was used to monitor the seeded batch crystallization of potassium sulfate and to calculate the resulting particle size distribution where mean particle diameter was ranging from 50-100 μm (Hipp et al., 2000).

Particle dynamics, such as flocculation and in result creaming in emulsions, can also be monitored using ultrasonic techniques. The concentration profile of emulsions droplets may change spatially and temporally, depending on the effective particle size and physical properties of the continuous (e.g., viscosity) and dispersed phases (e.g., density contrast to liquid phase). Pinfield et al. (1994) used ultrasonic measurements and compared them to concentration profile simulations in a creaming emulsion to follow depletion flocculation in oil in water emulsions containing a non-ionic surfactant. Similarly, in another work (Chanamai et al., 2000), ultrasonic properties over a frequency range of 1-150 MHz, apparent viscosity, and creaming rates of flocculated and nonflocculated 14% silicone oil-in-water emulsions were combined to collect more

realistic information about the floc structure and dynamics, which could not be accessed by using these techniques individually.

For characterizing the dispersions of large size crystals, often the case in many food systems, microscopic theories are generally insufficient. Empirical approaches, based on the bulk properties of system and characteristics of the components of the dispersion, can be more practical than microscopic scale mechanistic models (i.e., scattering models). Although Urick equation is classified among the scattering theories, its use is empirical in practice and considers the concentration measurements in crystal dispersions. Pinfield et al. (1995) showed that the Urick equation can also be derived as a special case of ECAH theory. The researchers made an adjustment on Urick equation by utilizing a calibration chart to be used at high volume fractions of the dispersed phase, and applied it to monitor the spatial and temporal change of concentration in a creaming emulsion (i.e., 20 wt% sunflower in oil emulsion with 2 wt% Tween20 and 0.03 wt% xanthan). Singh et al. (2002) used the Urick equation to determine the solid fat content (SFC) in different fat systems, anhydrous milk fat, cocoa butter, and their blends with canola oil (0-30 wt%). They found that the ultrasonic measurements are not in agreement with simultaneous pulsed NMR measurements. This discrepancy was attributed to the polymorphic difference of the crystalline fat which they speculated affected the ultrasonic properties. Saggin and Coupland (2004) followed a similar approach and used the Urick equation to measure SFC of coating fat in oil dispersions (2.5-12.5 wt%). In a similar manner to Pinfield et al. (1995), they showed the velocity is linearly related to SFC. Sayan and Ulrich (2002) correlated measurements of ultrasonic velocity to particle size (250-500 μm) and density of several salt suspensions. They noted a linear relationship between the density of salt dispersions and ultrasonic velocity with deviations only for larger particles, which could be attributed to the mixing imperfections.

In addition, ultrasonic attenuation can also be used empirically to follow concentration change empirically. Bamberger and Greenwood (2004) used ultrasonic attenuation measurements at a single frequency (i.e., 2.25 MHz center frequency) for real-time *in-situ* measurements of concentration of a silicon dioxide-water slurry (i.e., density of the fully

mixed slurry is 1270 kg/m^3) during a mixing process as a function of height in a stirred tank. The attenuation measurements were converted to concentration from a pre-prepared calibration.

Another technique to evaluate dispersion properties is ultrasonic reflectance measurements. Saggin and Coupland (2002) used measurements of the proportion of an ultrasonic wave reflecting from the interface between the container and the sample to characterize sugar (i.e., sucrose and lactose) dissolution. They found the reflected wave amplitude was sensitive to the dissolved solution composition but not the amount of undissolved material. They hypothesized that as the reflected signal is sensitive to only about the first wavelength of material it is reflecting from (~0.3 mm) which is depleted with respect to the large particles used and not be representative of the bulk. A complementary technique can be the monitoring of changes in dispersion properties during a phase change process (i.e., crystallization or dissolution). For example, Omar and Ulrich (1999) used ultrasonic velocity measurements to monitor supersaturation in an industrial crystallizer.

Saggin and Coupland (2004) used longitudinal and shear ultrasonic waves simultaneously for complete characterization of solid fat dispersions. They showed for a wide size range of crystalline particles that longitudinal ultrasonic properties are linearly related to solid fat content, whereas only attenuation is affected by crystal morphology and microstructure. Martini et al. (2005) considered a similar system to that of Saggin and Coupland (2004) and attempted to simultaneously investigate the effects of crystal size (i.e., determined by optical microscopy), and concentration (i.e., solid fat content was determined by pulsed-NMR) during unseeded isothermal crystallization of fats on ultrasonic parameters. The induction time for crystallization was also measured by ultrasound, and compared to turbidity measurements. They claimed that size of the solid fats affects the measured attenuation at only intermediate concentrations (i.e., 5-20%). However, their control and measurements for the crystal size and morphology were only based upon microscopic analysis.

Other than attenuation due to the scattering effects from individual crystals and the phase change process itself, some artifacts of the system may affect it. For example, high ultrasonic attenuation in frozen sucrose solutions (25-50 wt%) was attributed to the presence of air pockets entrapped within ice, rather than phase change itself, while ultrasonic velocity linearly changed with ice content (Gulseren and Coupland, 2008). In another study Holmes et al. (2007) used a model food system (i.e., olive oil, sucrose, and tripalmitin mixture) to monitor chocolate tempering process. They claimed that scattering from tripalmitin crystals dispersed in olive oil cannot be evaluated separately in the presence of high concentrations of sucrose crystals, and similarly the presence of seed crystals did not increase acoustic attenuation measurably in a frequency range of 1-12 MHz.

Chapter 2

STATEMENT OF THE PROBLEM

Many industrial processes depend on formation (via crystallization or dispersion) or destabilization (via dissolution or aggregation) of suspensions of crystals in liquids. Ultrasonic sensors, which can readily be applied as on-line (i.e., with minimal lag time for the sensor response and less labor intensive), non-invasive (i.e., without disturbing the process), non-destructive (i.e., without affecting the sample), flexible (i.e., allowing the measurement configuration to be modified according to the need), rapid, and inexpensive monitoring tools, are potentially useful to characterize these processes (Coupland, 2004).

I hypothesize that changes in ultrasonic sensor response can be used to determine changes in bulk properties (i.e., composition, particle size distribution) of suspensions of sugar crystals (i.e., lactose or sucrose) in a continuous liquid phase (i.e., water or vegetable oil).

There are three related objectives in this study:

1. The first objective was to use ultrasonic measurements to measure the composition of lactose-water mixtures (i.e., either solution or suspension) at equilibrium in terms of total lactose concentration and crystal load.
2. The second objective was to follow the kinetic changes in two related processes, i.e., dissolution and crystallization of lactose.
    a. The dissolution of lactose crystals and consequent changes in the system properties (i.e., crystal load, solution concentration) were monitored continuously and non-invasively by ultrasonic attenuation measurements and compared to off-line refractive index measurements. The rate of dissolution was tuned by varying the degree of under-saturation.
    b. The bulk crystallization of lactose from gelatin-lactose systems were monitored by ultrasonic measurements and compared to turbidity measurements. Isothermal differential scanning calorimetry (DSC) was

also used as a secondary control tool. Induction time and crystallization rates were compared for varying degrees of super-saturation and gelatin concentrations.

3. The third objective was to use ultrasonic attenuation measurements to monitor the mixing of sugar crystals (i.e., sucrose) into a lipid phase (i.e., corn oil), and follow (de)agglomeration during mixing. The degree of agglomeration was tuned by varying water concentrations as confirmed by solid bed volume measurements. Subsequent sedimentation kinetics at the cross-section of beam path was also monitored continuously by ultrasonic attenuation measurements.

Chapter 3

ULTRASONIC CHARACTERIZATION OF LACTOSE DISSOLUTION

3.1. Abstract

The ultrasonic properties (at 2.25 MHz) of lactose solutions and suspension of lactose crystals (d~50 μm) were measured as a function of concentration (0-40 wt%). Ultrasonic velocity increased linearly with concentration regardless of the state of dissolution of the lactose crystals while ultrasonic attenuation was low and concentration-independent when the lactose was dissolved and increased approximately linearly with the concentration of suspended crystals. Therefore the amount of lactose present and the state of dissolution can be determined simultaneously with single ultrasonic sensor. A sensor based on this principle was applied to a stirred tank and used to measure the time taken to mix powdered lactose into a solution and the time for the added lactose to dissolve.

3.2. Introduction

Many food preparation processes involve either the dissolution of crystalline ingredients in a solvent or the reverse process (e.g., dissolution of sugars and minerals, crystallization of lipids). In both cases the phase transitions are thermodynamically driven but kinetically limited. Crystallization requires two separate processes, nucleation and growth, whose rates are affected by the presence of nucleation catalysts and by factors affecting heat and mass transfer (Garside, 1985). Dissolution is the opposite of growth but as it does not require a nucleation event the rate is only affected by changes in heat/mass transfer (Ulrich, 2003). Both dissolution and growth can be slow and rate limiting to an overall process. Furthermore, because the kinetics of both crystallization and dissolution are affected by small variations in reaction conditions it is often necessary to allow more than the minimum process time required to ensure the transition has proceeded sufficiently. On-line sensors to measure the amount of crystalline vs. dissolved material would allow greater control of the process and thus increase efficiency.

Existing methods to measure the dissolution (or crystallization) kinetics of small molecules typically involve separating the crystal and solution phases and measuring the amount of solute in either (e.g., by filtering and measuring the solution concentration by optical rotation or refractive index) (Haase and Nickerson, 1966a, 1966b; Raghavan et al., 2001; Ziegler et al., 1987). However because these processes require a physical separation of the crystal from solution phase they are often difficult to apply on-line. It is also possible to determine the presence of dispersed crystals by light scattering (Mimouni et al., 2005). Finally, nuclear magnetic resonance (NMR) can measure the environment of certain nuclei and, from that, infer the balance of phases present. However, NMR methods are often relatively slow and expensive and cannot make measurements inside metal containers. Ultrasound may serve as an ideal method which would be rapid and could be conducted on-line without disturbing the process and give a rapid automat to probe the bulk properties of the system.

Ultrasound is a mechanical wave with frequencies above the range of human hearing (>20 kHz). When used in sensing application, the frequencies used are typically in the megahertz range and the wave amplitude is low, so the material deformations are small and non-destructive (Povey, 1997; Coupland, 2004). The capacity of a material to transmit sound can be described in terms of ultrasonic velocity (i.e., time to travel unit distance) and attenuation coefficient (i.e., logarithmic loss of wave energy per unit distance traveled). Ultrasonic properties are related to the physical properties of the material as:

$$\frac{\omega}{k} = \sqrt{\frac{M(\omega)}{\rho}} \qquad (3.1)$$

where ω is the angular frequency (=2πf, where f is the ultrasonic frequency), k is the complex propagation coefficient (=ω / c + iα, where c is ultrasonic velocity, α is the attenuation coefficient and i is √-1), ρ is the density and M is the complex elastic modulus of the material supporting the sound wave. Density and modulus are readily related to changes in composition and structure which provides the physical basis for the use of ultrasound as a sensor. In complex fluids where one material is suspended in a second, the situation becomes more complex as the particles can scatter sound in a frequency-dependent manner (Povey, 1997). Ultrasonic spectroscopy has been used to measure the size distribution of emulsions and colloidal dispersions with by means of well-established scattering theories relating the measured ultrasonic properties with the physical properties of the suspension (Challis et al., 2005; McClements and Povey, 1989; Tebbutt and Challis, 1996). This approach has been used to a lesser extent to characterize crystal dispersions.

Sayan and Ulrich (2002) correlated measurements of ultrasonic velocity to particle size and density of several salt suspensions while Omar and Ulrich (1999) used ultrasonic velocity measurements to monitor supersaturation in an industrial crystallizer. Ultrasonic attenuation spectroscopy was also used to monitor the seeded batch crystallization of different salt solutions (Hipp et al., 2000) and also for size characterization of

homogenous particles and emulsions as well as porous particles in the micrometer range (Richter et al., 2006). Saggin and Coupland (2002) used measurements of the proportion of an ultrasonic wave reflecting from the interface between the container and the sample to characterize sugar dissolution. They found the reflected wave amplitude was sensitive to the dissolved solution composition but not the amount of undissolved material. They hypothesized that as the reflected signal is sensitive to only about the first wavelength of material it is reflecting from (~0.3 mm) it is depleted with respect to the large particles used and not be representative of the bulk.

The existing methods for tracking crystallization/dissolution processes on-line all have characteristic limitations. Sensors based on ultrasonic methods have shown some promise but there has been no attempt to integrate velocity and attenuation measurements with a goal of simultaneously measuring composition and crystal load as well as monitor the kinetics of dissolution. The model systems used in this study are solutions and dispersions of lactose crystals in water. Lactose is a commonly used food ingredient as well as a tableting material for pharmaceuticals (Raghavan et al., 2001). The presence of lactose crystals is associated with defects to certain dairy products (e.g., sweetened condensed milk, ice cream and processed cheese). The kinetics of dissolution of α-lactose monohydrate crystals follows a two step-process (Hunziker and Nissen, 1926). A small amount of lactose dissolve almost instantaneously quickly reaching the solubility limit of the α-polymorph. Further crystal dissolution can only occur as some of the dissolved α-lactose mutarotates to the β-form. Thus the overall dissolution kinetics is often limited by the rate of mutarotation.

3.3. Methods and materials

α-Lactose monohydrate (reagent grade) was purchased from Sigma-Aldrich (St. Louis, MO) and used without modification. The crystals were characterized by optical microscopy (Olympus BX-41, Hitech Instruments, Edgemont, PA; 20X) equipped with a SPOT Insight QE camera (SPOT Diagnostic Instruments, Sterling Heights, MI) and by static light scattering (Horiba LA-920, Irvine, CA assuming a relative refractive index of

1.11 with an imaginary part as 0.01) after dispersed in 2-propanol (>99.5%, Sigma Aldrich) to avoid multiple scattering effects.

Preparation of lactose suspensions. Aqueous lactose solutions and suspensions (0-40 wt% along with 0.01 wt% thermirosal to prevent microbial spoilage) were prepared by allowing the ingredients to come to equilibrium in water at 37°C for 3-4 days. During the storage, samples were shaken occasionally, and equilibrium was confirmed by refractive index measurements. Supersaturated solutions were prepared by heating the mixtures to 65°C for about 10 minutes to allow complete dissolution then cooling back to 37°C. The supersaturated solutions were stable over the time course of the experiment so it was possible to compare their ultrasonic properties with those of lactose crystal suspensions in saturated lactose solutions. All measurements were performed at 37°C. Temperature was controlled by immersing the sample containers in a stirred waterbath controlled to ±0.01°C and confirmed by thermocouple measurements inside the sample to be within 0.1°C of the target temperature. The one exception to this was when powders or solutions were added to the mixed tank, there was a small change in temperature despite previously bringing the added sample to approximately the same temperature. However these changes were small (<0.5 °C) and the sample returned to within 0.1 °C of the set point within 1-2 min (as measured by a thermocouple inside the sample.) The temperature fluctuation could lead to a change of perhaps 1-2 ms^{-1} in the reported velocity data but this is insufficient to be seen in the figures or to influence the conclusions drawn.

Solution concentration was measured by refractive index by using a temperature controlled refractometer (Reichert, Arias 500, NY). In preliminary work I showed that refractive index (RI) was proportional to lactose solution concentration (C, wt%) (RI = 1.332 + 0.0015C, $R^2 = 0.999$, see Appendix A.1) and this calibration was used as a reference method to measure dissolution kinetics.

Ultrasonic measurements. Initial ultrasonic characterization of the lactose samples was performed using a high-precision ultrasonic pulse-echo reflectometer (McClements and Fairley, 1992) (Figure 3.1a). An electrical spike signal (Panametrics 500 PR, Waltham,

MA) was passed to a 2.25 MHz broadband ultrasonic transducer (Panametrics V606), which converted the energy to ultrasound. Fourier analysis of the ultrasonic signal showed a bell-shaped frequency composition with a center frequency of 2.2 MHz and a half-height peak width of 1.6 MHz. The pulse of sound traveled into a Plexiglas delay line, and was partially reflected at the planar interface with the sample. The reflected part returned through the delay line to the transducer (echo 1) and the transmitted part traveled through the sample (~1 cm), was reflected from a brass plate and returned through the sample and the delay line to the transducer (echo 2). The transducer reconverted the acoustic signal to an electrical signal, which was stored for analysis with a digital oscilloscope (LeCroy 9310c, Chestnut Ridge, NY). The time and energy difference between the echo 1 and echo 2 were used to calculate the speed of sound and attenuation, respectively.

In other experiments, a thermostated and stirred tank was fitted with ultrasonic sensors to more closely reproduce processing conditions (Figure 3.1b). The same electrical components were used although in through-transmission mode with one transducer generating sound pulses and the second on the other side of the container receiving them. Data acquisition was automated using LabView (version 7.1, National Instruments, Austin, TX) to allow collection periods as low as 0.1 s. The sample container in this case was a cylinder (internal diameter 10.4 cm) agitated with a blade stirrer (5 cm diameter and 1.3 cm width with 0.6 cm diameter shaft) driven at 500 rpm by a laboratory scale stirrer (STIR PAK laboratory stirrer, Model 4554, Cole Parmer, Chicago, IL). The cell was calibrated by measuring the time of flight and power of an acoustic pulse passing through water (t_{water}, I_{water}) respectively then the speed of sound and attenuating properties of the sample were calculated from similar measurements in the sample (t_{sample}, I_{sample}):

$$c_{sample} = \frac{c_{water}}{t_{water}} \times t_{sample} \qquad (3.2)$$

$$\text{NPTL} = 10 \log (I_{water} / I_{measured}) \qquad (3.3)$$

where c_{water} is the speed of sound in water (=1523.93 ms^{-1} at 37°C, Bilaniug and Wong, 1993) and NPTL is the normalized power transmission loss (a measurement of attenuation). Transmitting ultrasound across this longer distance causes additional power loss due to beam spreading (diffraction) (Povey 1997). However by normalizing the results to those of water these effects are minimized.

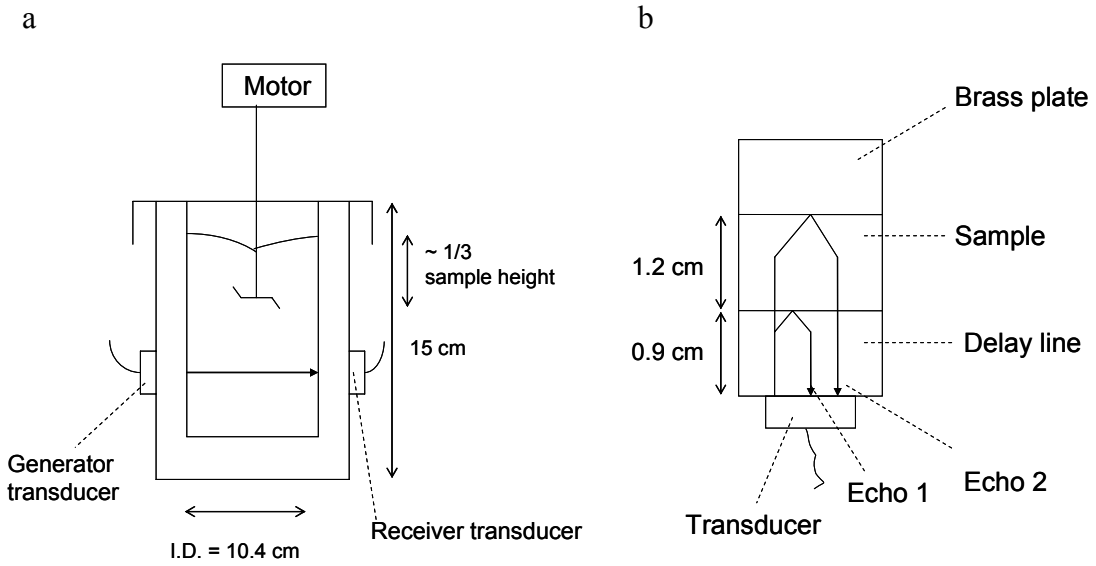

Figure 3.1. Diagrams showing (a) the ultrasonic pulse echo reflectometer and (b) the stirred tank configuration of transducers. Both devices measure velocity from the time taken for sound to travel a known distance between two transducers (or reflect and return to the same transducer) and attenuation as the loss of pulse energy after travelling a known distance through the sample.

3.4. Results and discussion

3.4.1. Characterization of lactose and lactose suspensions

The mean size of the lactose crystals was 50 μm as determined by light scattering (Figure 3.2a). The crystals seen under the microscope (Figure 3.2b) were approximately this size and were angular and irregularly shaped with only a relatively small proportion corresponding to the typical "tomahawk shape" of α-lactose monohydrate crystals obtained from aqueous solutions (Hunziker and Nissen, 1927). This asymmetrical morphology has been attributed to the influence of the impurity β-lactose (Raghavan et al., 2002). The crystals are an order of magnitude smaller than the wavelength of sound used (677 μm in water). The solubility limit of lactose in water at 37°C was determined by allowing excess crystals to come to equilibrium with water over several days and the measured result (24 wt%) was similar to literature data (24 wt% at 39°C, Hudson, 1908).

a

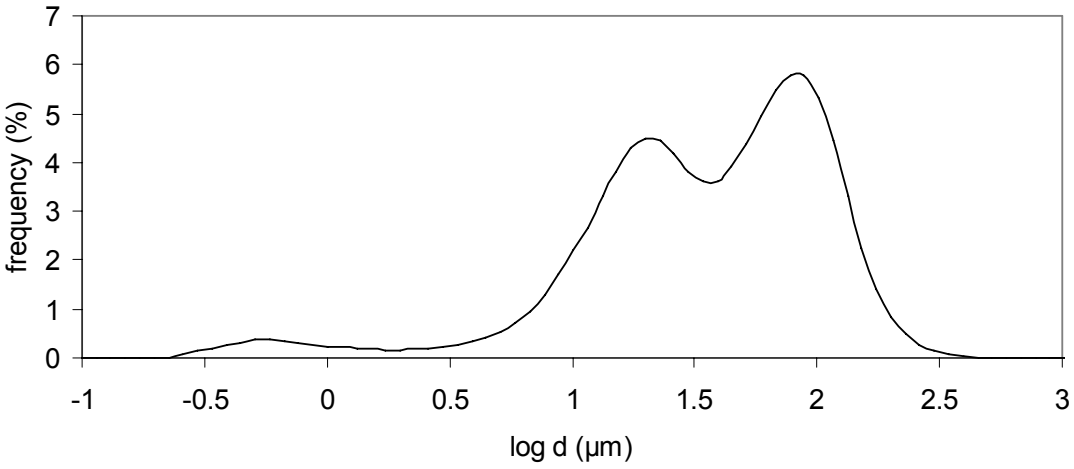

b

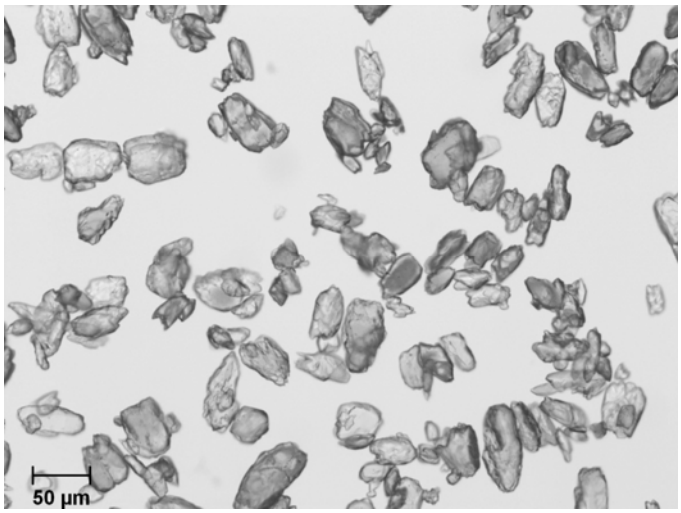

Figure 3.2. (a) Particle size distribution and (b) micrograph of the lactose crystals used.

The ultrasonic properties of lactose-water mixtures were investigated using the analytical measurement cell configuration. The ultrasonic velocity increased steadily with concentration and there was no break in the curve corresponding to the solubility limit (Figure 3.3a). The ultrasonic velocity in lactose crystal dispersions was compared to supersaturated solutions of the same composition (prepared by heating the suspensions until the crystals dissolved then re-cooling to 37°C) and there were no differences. Therefore, ultrasonic velocity was sensitive to the amount of lactose in the container but not to its state (i.e., super-saturated solution vs. a mixture of saturated solution and suspended crystals). Therefore a measurement of ultrasonic velocity could be used to measure the total amount of lactose present but I would not expect any changes in velocity during dissolution or crystallization process provided crystals were uniformly distributed across the beam path. Sayan and Ulrich (2002) also noted a linear response between the density of salt dispersions and ultrasonic velocity with deviations only for larger particles. It should be noted that this observation, while valid for this system, is unlikely to be universal. Fine particles scatter sound in a frequency and particle size dependant manner (Povey 1997) and it seems likely that other combinations of crystal size and ultrasonic frequency would give greater or smaller changes in velocity on dissolution.

The ultrasonic attenuation coefficient was low and effectively independent of composition for all sub-saturated solutions and also for supersaturated solutions. However, when crystals were present the attenuation coefficient increased approximately linearly with crystal load (Figure 3.3b). It should be noted that there was considerable error in the determination of attenuation coefficient in the crystal suspensions, especially for higher crystal loads, probably due to difficulties in maintaining adequate mixing.

a

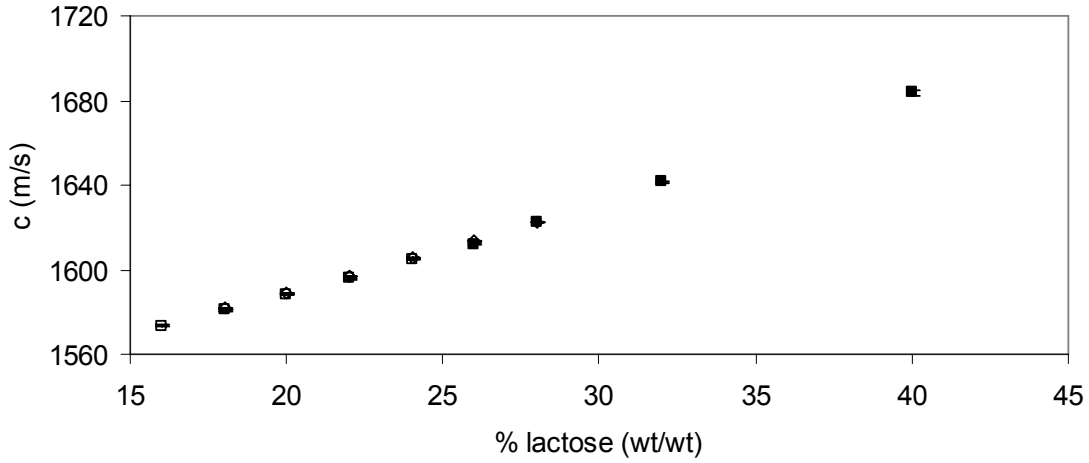

b

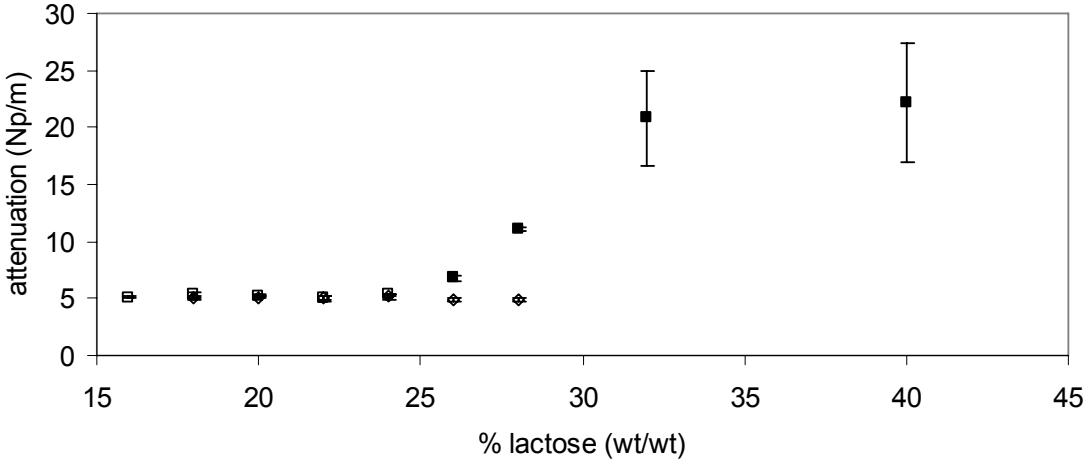

Figure 3.3. Ultrasonic (a) velocity and (b) attenuation coefficient of lactose solutions (open symbols) and suspensions (filled symbols). Measurements were conducted using a 2.25 MHz center frequency transducer in a pulse echo reflectometer. Points and error bars are the mean and standard deviation of three experimental replications, respectively.

3.4.2. Validation of ultrasonic measurements in the stirred tank apparatus

From these preliminary measurements, it appears a combination of ultrasonic attenuation and velocity measurements can be used to measure the concentration of lactose crystals and the overall composition (crystal plus solution) simultaneously. However, although the analytical cell gave precise data it was not a realistic representation of a processing vessel and it was also difficult to maintain crystals in suspension. Consequently, we designed and built a stirred tank mixed tank with integral ultrasonic sensors to test these sensing principles in a more realistic process environment. The device provides similar measurements to the instrument developed by Titiz-Sargut and Ulrich (2003) for characterizing crystal dispersions but in my case the sensors are integrated with the container walls to minimize process disruption and there is no screen to exclude large particles so the measurements is more representative of the overall suspension.

Preliminary experiments showed the mixer was sufficient to keep the lactose crystals adequately distributed and the rate of mixing did not affect the ultrasonic properties of the samples. The operation of the device was tested by measuring the ultrasonic velocity and attenuation of lactose solutions and suspensions similar to those studied earlier and once again, the speed of sound increased linearly with lactose concentration regardless of whether the sugar was dissolved or not and there was no difference between measurements in two configurations used (Figure 3.4a). The trends in transducer loss (NPTL) for solutions and suspensions in the stirred tank (Figure 3.4b) mirrored the trends in attenuation coefficient for similar samples measured in the pulse echo reflectometer (Figure 3.3b). Note that the very slight decrease in NPTL with increased dissolved lactose concentration was mainly due to the changed impedance of the solution slightly decreasing the losses due to reflections at the sample-wall boundaries.

a

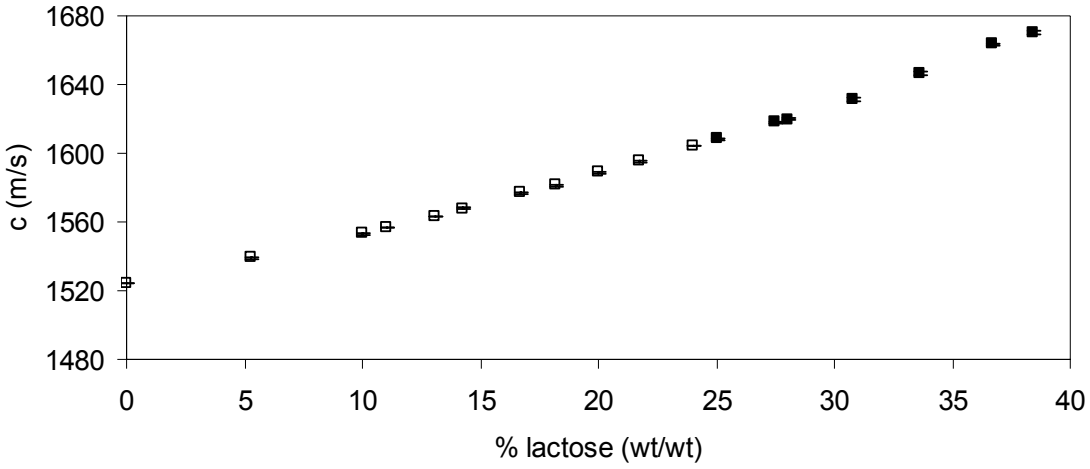

b

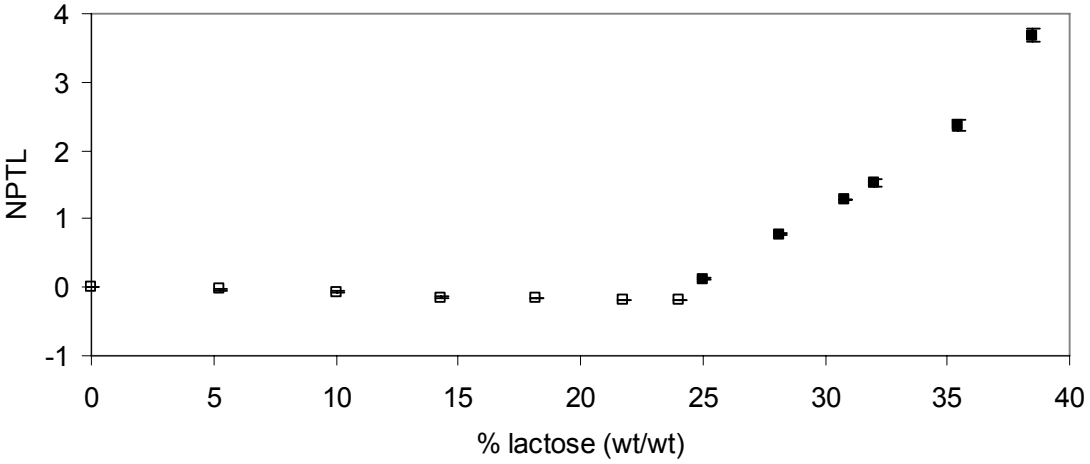

Figure 3.4. Ultrasonic (a) velocity and (b) transducer loss of lactose solutions (open symbols) and suspensions (filled symbols). Measurements were conducted using a pair of 2.25 MHz center frequency transducers in through-transmission mode in a stirred tank configuration. Points and error bars are the mean and standard deviation of three experimental replications, respectively.

3.4.3. Kinetics of Mixing and Dissolution

Having established the stirred tank configuration could be used to reliably measure the ultrasonic properties of defined lactose solutions and suspensions, the next series of experiments were an attempt to follow the dissolution process ultrasonically. Powdered lactose (pre-heated to 40°C to minimize temperature changes) was added to lactose solution at 37°C in the stirred tank and the ultrasonic properties measured at 100 ms intervals throughout the mixing and dissolution process. Small samples (~2 mL) were withdrawn at intervals, filtered through a 0.2 μm syringe filter, and the dissolved lactose concentration determined from a refractive index measurement.

Clearly when powdered lactose is added to water there are (at least) two processes occurring that could potentially affect the ultrasonic signal: mixing and dissolution. To separate these effects, I conducted two series of experiments:

3.4.3.1. Mixing without dissolution

In these measurements lactose powder was mixed with a saturated lactose solution so the changes seen are due to mixing without any possibility of crystal dissolution. In this case NPTL increased quickly and then returned to a steady state after about 2 minutes which constituted a mixing time (Figure 3.5a). In other experiments (see below) when liquids were added to liquids the mixing time was greatly reduced leading us to propose that the attenuation peak seen here is due to the incorporation and dissipation of air bubbles entrained within the dry powder rather than inhomogeneities in the crystal suspension itself. During the mixing time it was not possible to make accurate measurements of the state of crystal dissolution and so constitutes a “dead time” for the instrument. It does however provide a useful measure of the time required for mixing to be complete. There was some variation in ultrasonic velocity immediately after lactose addition as the system was mixed and contaminated with air bubbles within the powder but then remained unchanged throughout the dissolution. This was expected as there was no difference in

ultrasonic velocity between a lactose solution and crystal suspension of the same composition and velocity measurements are not reported or discussed further.

3.4.3.2. Mixing and dissolution

In these measurements lactose powder was added to undersaturated lactose solutions to allow simultaneous mixing and dissolution. NPTL increased immediately upon lactose powder addition before decreasing initially rapidly then more slowly (Figure 3.5b). After approximately 3 min the NPTL was almost constant suggesting dissolution was complete (contrast with the 2 min dead time for the “just mixing” experiment, Figure 3.5a). The same dissolution process was tracked with offline refractive index measurements (Figure 3.5b) and reached a steady state at about the same time as the ultrasonic sensor. However, in this case, because the time for mixing was comparable to the time for dissolution it was not possible to extract any useful information on dissolution kinetics.

a

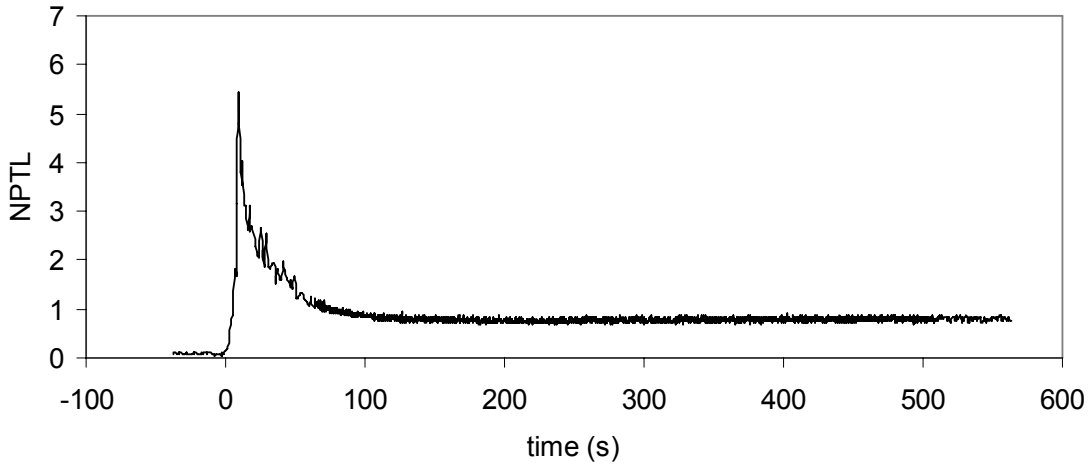

b

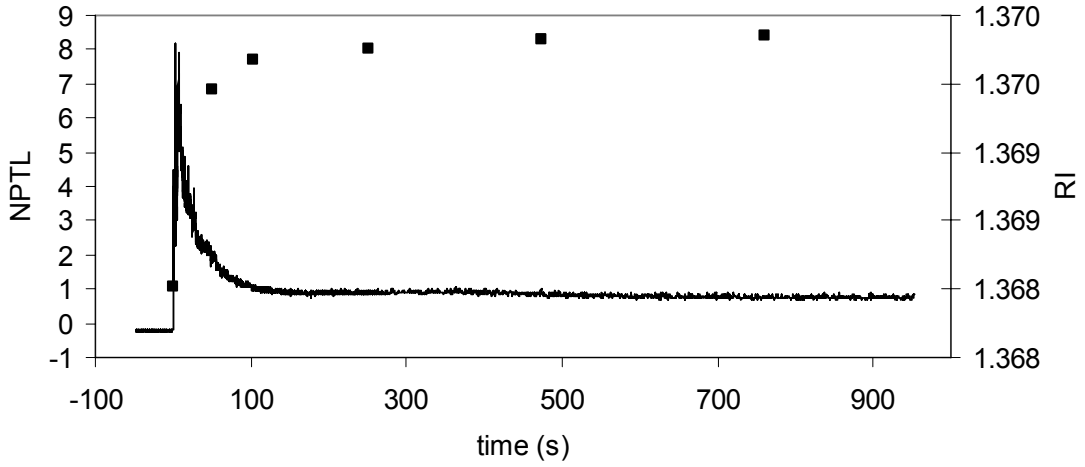

Figure 3.5. Kinetic changes in transducer loss (NTPL) on increasing lactose amount by adding lactose powder in a stirred tank configuration. Lactose was added at time = 0. (a) Mixing without dissolution. Powdered lactose (50 g) was added to a lactose suspension (1200 g of a 25% mixture, i.e., a suspension of 1% lactose crystals in a 24% lactose solution) yielding a final composition of 28 wt% (i.e., 4 wt% crystal load) . (b) Simultaneous mixing and dissolution. Powdered lactose (66.0 g) was added to lactose solution (950 g, 23%) yielding a 28% lactose mixture (i.e., 4% suspended lactose). Off-line refractive index measurements at discrete intervals are shown on the right hand axis.

In my final series of experiments I modified the mixing protocol to minimize the dead time and allow a more realistic determination of dissolution kinetics. Water was added to suspensions of lactose crystals in saturated lactose solution in the stirred tank and dissolution was measured on-line by ultrasonic measurements and off-line by refractive index. As in previous experiments, the process involved both mixing and dissolution so I had to first establish the dead-time during which mixing effects dominate. This was done by adding saturated lactose solution instead of water to the lactose suspension in the tank to eliminate any dissolution (Figure 3.6a). In this case, the dead time was much shorter (taken conservatively as 30 seconds), probably because little or no air was incorporated during the mixing of liquids. When water was added to lactose suspensions under the same mixing conditions then the signal changes after the dead time were taken as representative of the dissolution process (Figure 3.6b). Over this period both solution concentration and transducer losses changed approximately exponentially with time and so, the dimensionless change in sensor response, I, was modeled as:

$$I = \frac{I_t - I_\infty}{I_o - I_\infty} = e^{-kt} \qquad (3.4)$$

where I_t is the response of the sensor (either refractive index or NPTL) at time t, at the beginning of the experiment (subscript 0) or at equilibrium (subscript ∞) and k is the effective rate constant for dissolution. Because of the dead time during mixing for the ultrasonic measurement only data recorded after this period were included and (I_0-I_∞) was determined as a fitting parameter in the model.

a

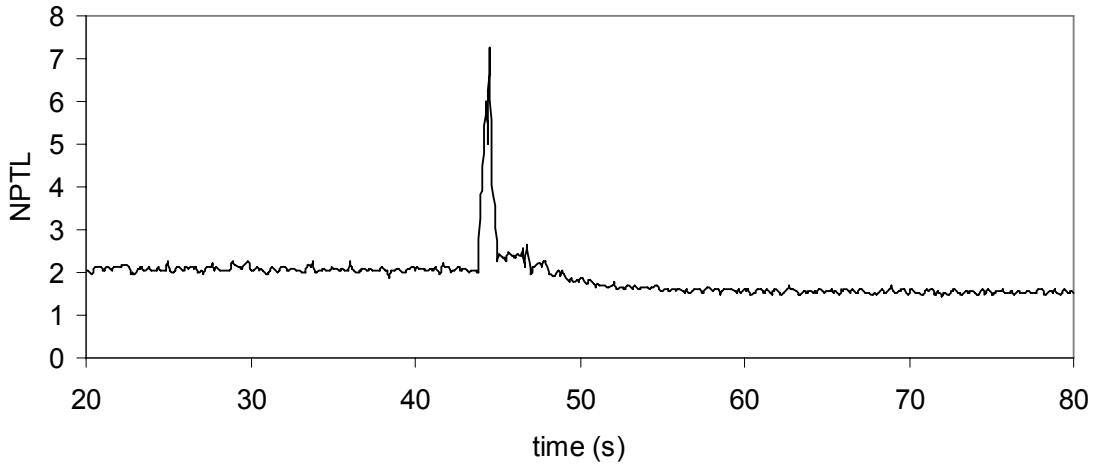

b

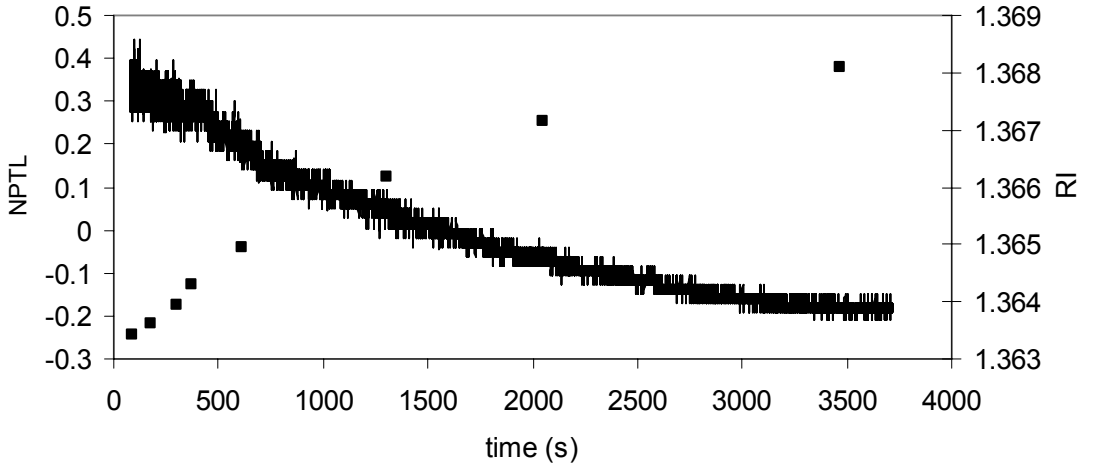

Figure 3.6. Kinetic changes in transducer loss (NTPL) on decreasing lactose concentration in a stirred tank configuration (addition at time = 0). (a) Mixing without dissolution. Saturated lactose solution (400 g) was added to 920 g lactose suspension (32 wt%) decreasing the crystal load to about 6 wt%. (b) Simultaneous mixing and dissolution. Water (373.1 g) was added to lactose suspension (953.5 g, 32 wt% lactose, i.e., 8% crystal suspension) yielding an undersaturated solution (23 wt%). Off-line refractive index measurements at discrete intervals are shown on the right hand axis.

The results from the regression analysis are presented in Table 1 (note that as refractive index increased during dissolution while NPTL decreased the signs of the calculated rate constant are different although I hypothesize the process being described is the same). The model fitted the data well with a standard error was less than 0.001 and a correlation coefficient greater than 0.99 in each case. The rate constants measured by ultrasound were all statistically similar to one another regardless of the initial lactose concentration. This is as expected because although the overall dissolution rate increases with degree of undersaturation the process, and hence rate constant, remains the same. However, when dissolution was characterized by refractive index measurements the dissolution rate decreased with increases in understauration. Although a similar trend was also observed in ultrasonic measurements, the rate constant did not change significantly. There can be several reasons causing this difference. For example, lower sampling rates of refractive index measurements compared to ultrasound may have affected the model efficiency, or the time lag associated with making an off-line measurement decreased the reliability of refractive index measurements. On the other hand, ultrasonic measurements can be affected from the changes in particle size distribution during dissolution, and hence this may have affected the calculated rate constant for the dissolution process. The calculated rate constants are in reasonable agreement with values reported in the literature using a mutarotation method (88×10^{-5} s^{-1}, Haase and Nickerson, 1966a).

The dissolution process was also compared in a monitoring technique-wise manner (Table 1). Although the rate constants for the two methods were similar, the highest and lowest initial concentrations resulted in significant difference. In addition to the limitations of the two techniques, the reason for this difference can be coming from the dissolution dynamics of lactose. Since the dissolution of lactose is characterized by two subsequent processes as the instantaneous initial solubility (i.e., determined by the solubility of α-lactose) and much slower equilibrium solubility (i.e., determined by the equilibrium mutarotation ratio), the calculated effective rate constant was modified with changing degree of dilution.

Table 3.1. Rate constant for lactose dissolution calculated from ultrasound and refractive index measurements as a function of initial lactose concentration. Data are shown as the mean and standard deviation of three full experimental replicates. Different letters show significant difference within a measurement technique, while roman numbers were used to compare the similarity of the techniques for the same concentration ($p<0.05$).

[lactose] /wt%	**Dissolution rate constant (10^{-5} s^{-1})**	
	ultrasound	-RI
30	$74.6\pm6.5^{a,I}$	$85.5\pm2.2^{a,II}$
32	$72.1\pm0.1^{a,I}$	$75.8\pm4.5^{b,I}$
34	$68.5\pm2.5^{a,I}$	$69.3\pm0.6^{bc,I}$
36	$69.5\pm0.9^{a,I}$	$66.3\pm0.9^{c,II}$

3.5. Conclusion

The increase in ultrasonic velocity (relative to water) is proportional to the amount of lactose in the sample regardless of the state (dissolved or crystalline). Ultrasonic attenuation is low when the lactose is dissolved but increases approximately linearly with undissolved lactose concentration. Combination of velocity and attenuation measurements can therefore be used to estimate both the amount and state of the lactose and thus progression of processes such as dissolution and crystallization. The ultrasonic method is ideal for application as an on-line sensor as it can be applied non-invasively and can give robust and rapid results. Furthermore, the high sensitivity of ultrasonic attenuation to inhomogeneity within the sample makes it a potential method to measure the progress of a mixing operation (e.g., conching of chocolate).

It should be stressed that the approach pursued here is entirely empirical. It should be possible to devise a more complete description of the wave-matter interactions using scattering theory especially as the system is in the long wavelength limit, i.e., the wavelength of sound (~600 μm) >> particle size (~50 μm). Furthermore, by taking measurements over a range of ultrasonic frequencies it should be possible to simultaneously calculate the size of the particles present.

Chapter 4

ULTRASONIC CHARACTERIZATION OF LACTOSE CRYSTALLIZATION IN GELATIN GELS

4.1. Abstract

Since ultrasonic waves are sensitive to the bulk properties (i.e., density and compressibility) of a homogenous system (e.g., solution), and are often modified by the characteristics of the different phases in a dispersion, they can be used to follow kinetic changes in a dispersion, such as crystallization. Ultrasonic velocity and attenuation measurements (2.25 MHz center frequency) were used to follow bulk crystallization of lactose from gelatin gels at 25°C, and compared to turbidity (500 nm) and calorimetry measurements.

Ultrasonic attenuation measurements were shown to be more sensitive to the crystallization of lactose than ultrasonic velocity measurements. Two rate parameters were defined to compare the effects of formulation on the kinetics of lactose crystallization, a maximum rate (r_{max}) and induction time (t_i). All measurement methods showed similar trends with different formulations. With increasing lactose super-saturation, r_{max} increased and t_i decreased significantly ($p<0.05$) while the inhibitory effects of gelatin on crystallization kinetics were not significant. Although it is difficult to make conclusions about the relative effects of gelatin-lactose interactions on lactose crystallization, ultrasonic measurements were able to differentiate between different crystallization conditions and can be used for further analyses of the thermodynamics and kinetics of the water-lactose-gelatin system.

4.2. Introduction

Lactose is a disaccharide of glucose and galactose with two isomeric forms, α and β, that interconvert by motarotation and exist at equilibrium in solution. For example, in water at 20°C, 37.3% α-lactose and 62.7% β-lactose are present at equilibrium (Ganzle et al., 2008). Temperature changes have only a small effect on the equilibrium ratio of concentrations of the isomers (Whitaker, 1933), while the rate of mutarotation is profoundly affected by temperature (Whitaker, 1933; Haase and Nickerson, 1966a). When a lactose solution is super-saturated at moderate temperatures (below 95°C), α-lactose monohydrate crystals will be obtained since the α-form is less soluble and crystallization will continue so long as α-lactose in solution can be replenished by mutarotation. Haase and Nickerson (1966b) showed that the mutarotation rate is not limiting to crystallization at moderate temperatures (15-45°C). However at low temperatures (i.e., refrigeration temperatures) where the mutarotation rate decreased substantially (Whitaker, 1933), or in the presence of many crystal nuclei which increase the crystallization rate (Twieg and Nickerson, 1968) the mutarotation rate can be rate limiting to the overall crystallization process. In a similar manner, it was shown that surface incorporation of lactose crystals into the crystal lattice rather than molecular diffusion in the aqueous solution rate is limiting to crystallization (Haase and Nickerson, 1966b; Nickerson and Moore 1974).

Although crystallization rate generally increases with supersaturation, there are many other factors (e.g., impurities acting as crystallization inhibitors or catalysts) that can affect overall kinetics, as well as the final crystal morphology and microstructure. Depending on the crystallization conditions, the shapes of lactose crystals formed can vary (Ganzle et al., 2008). For example, when the crystallization is fast, only prism-shaped crystals are formed, and with decreasing degree of super-saturation diamond shaped plates, then pyramids and finally tomahawk shapes can be observed (Herrington, 1934). Lactose crystallization can be desirable (e.g., during refining from whey), or undesirable (e.g., in ice cream as it causes sandiness) so monitoring and control of the process is essential.

The crystallization of lactose can be affected by the presence of hydrocolloids including gelatin. Firstly, a gel environment can prevent any possible convective flow effects, which can modify heat and mass transfer processes, and can also eliminate secondary nucleation events due to the fragmentation of pre-existing lactose crystals. Secondly, in the presence of gelatin molecules may affect the phase equilibrium of the reaction. Gelatin is sometimes used to inhibit the sandiness defect due to lactose crystallization in ice cream (Nickerson, 1962). Some early studies (described by Whitaker, 1933, and Ganzle et al., 2008) showed that high gelatin concentrations (i.e., >1%) delayed lactose crystallization in ice cream at moderate but not high levels of lactose supersaturation.

In order to follow crystallization in a gel, it is difficult to separate individual crystals from solution for analysis and the monitoring technique selected needs to differentiate crystallization from other the changes in the solution phase. The process of crystallization can be monitored on-line using a variety of techniques including turbidity measurements. However, ultrasonic methods can be used for *in-situ* monitoring of crystallization process more effectively as they are applicable to optically opaque systems.

Acoustic waves propagate as a series of compressions and rarefactions and can change their properties depending on the nature of the media that they are travelling. Low intensity (i.e., deformations within the elastic limit of the material) ultrasound (>18 kHz) can be used to monitor phase change process in optically opaque solutions non-invasively and can readily be applied on-line (Coupland, 2004). Ultrasonic velocity and attenuation (i.e., the logarithmic loss of the wave energy with distance) measurements can provide physico-chemical information about the system (i.e., compressibility and density). When solid particles are present in a continuum, they will scatter sound in a frequency dependent manner. This scattering event or collection of different events can be observed as an additional energy loss (i.e., attenuation change) and a phase change in the measured wave (i.e., yielding velocity dispersion).

There have been attempts to use ultrasonic techniques to follow crystallization process. For example, the change in crystal size distribution during crystallization of copper (II) sulphate pentahydrate from bulk (Tebbutt et al., 1999) and seeded (Marshall et al., 2002) solutions were calculated from ultrasonic spectra using scattering theories. However, the results showed some deviation from light scattering measurements. Saggin and Coupland (2004) measured the amount of fat crystallized (i.e., solid fat content) of coating fat in oil dispersions (2.5-12.5 wt%) using ultrasonic attenuation and velocity measurements. Omar and Ulrich (1999) used ultrasonic velocity measurements to monitor the degree of supersaturation of K_2SO_4 solution in an industrial crystallizer during seeded crystallization. In Chapter 3, I showed that ultrasonic attenuation measurements were sensitive to the concentration of lactose crystals dispersed in a lactose solution, whereas velocity measurement only to the total lactose independent of its state. The objective of this study is to develop my earlier observations and in this case follow the kinetics of lactose crystallization.

4.3. Materials and methods:

Solution preparation: Gelatin from bovine skin (type B, 225 bloom) and α-lactose monohydrate (reagent grade) were obtained from Sigma-Aldrich and used without further modification. Lactose (43-46 wt%) and gelatin (1.5 and 3 wt%) were added to high purity water (Nanopure Barnstead, Dubuque, IA), and stirred for about half an hour at room temperature to allow the gelatin to hydrate. The samples were then heated to 75-80°C and stirred for a further 15 min to ensure complete dissolution.

Crystallization: Crystallization kinetics was monitored *in-situ* by ultrasonic measurements over several hours and the results were compared to off-line turbidity measurements made in similar samples. For ultrasonic measurements, an immersion probe configuration (Fig. 4.1) was dipped into a beaker containing 30 mL of the hot solution and immediately covered with several layers of Parafilm to prevent evaporation. For turbidity measurements, aliquots of the hot solution was sampled into 3 mL plastic cuvettes and sealed with plastic caps. The samples were cooled in a waterbath to

25.00°C±0.01°C. The solubility limit of lactose in water under these conditions is 18% so the samples prepared were 25-28 wt% super-saturated (Whittier, 1944). Thermal equilibrium was reached in about 10 minutes as confirmed by external thermocouple measurements (±0.1°C) in representative samples.

Ultrasonic measurement: Ultrasonic velocity and attenuation were measured using a custom-built high precision ultrasonic pulse-echo reflectometer (Fig. 4.1). This immersion probe has similar elements and configuration to the analytical measurement cell used in Chapter 3, yet modified to allow it to be immersed in the liquids to be analyzed. A 2.25 MHz ultrasonic transducer (Panametrics V606, Waltham, MA), used to generate and detect ultrasound, coupled (Couplant D, Gel Type, Panametrics) to a Plexiglas delay line, which was attached in parallel to a stainless steel reflector plate by thin rods. This configuration allows ultrasonic measurements by dipping the probe in a liquid and allowing the liquid to fill the gap between the delay line and the reflector plate. The operation of the device was identical to the measurements described in Chapter 3.

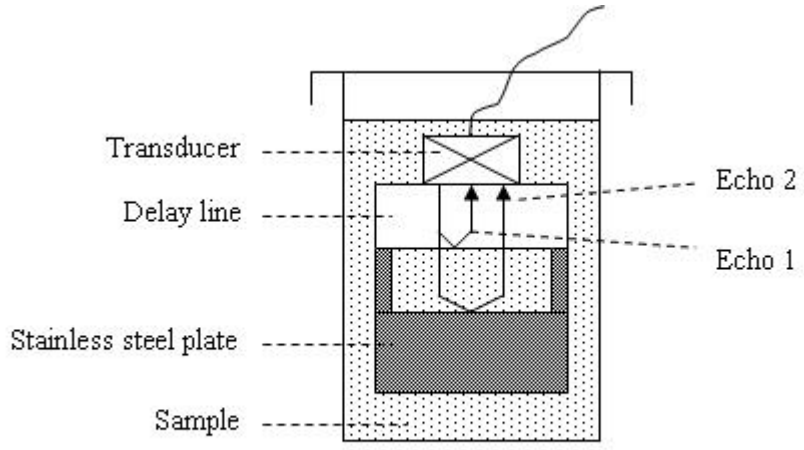

Figure 4.1. Immersable ultrasonic pulse-echo reflectometer.

Turbidity measurements: The crystallization kinetics was monitored by turbidity measurements (Spectronic 20 Genesys spectrophotometer, Spectronic Instruments Inc., NY). The cuvettes containing crystallizing solution were removed from the water bath at intervals and turbidity was monitored at 500 nm as compared to a gelatin blank.

Isothermal DSC: Heat is released during crystallization and can be measured by sensitive isothermal calorimetry. Samples (0.513 mL) were loaded into a microcalorimeter (VP-DSC, Northampton, MA) thermostated at 25°C. As soon as the equilibrium temperature was reached, the heat flux data was recorded with respect to that for the reference chamber filled with water. The effect of thermal changes in the gelatin component was minimized by subtracting a similar curve generated with a gelatin solution from the sample data prior to further analysis. In order to calculate the enthalpy of crystallization, DSC analysis requires the construction of an appropriate baseline. The baseline (Appendix B.2) was drawn as a straight line from the beginning of exothermic change (i.e., a negative change in the heat flow) to the final plateau indicating the end of crystallization yielding a single exothermic peak. The area under the isothermal DSC peak is due to the enthalpy released on lactose crystallization and the fraction of the total area released at any time was taken as the proportion of the lactose crystallizaed at that time (Foubert et al., 2003):

Crystal characterization: After 24 h, samples were removed for analysis of the crystals present. A small portion of the sample was gently pressed onto to a glass microscope slide, covered with a glass cover slip and sealed with a high viscosity immersion oil to prevent evaporation during analysis. An optical microscope (Olympus BX-41, Hitech Instruments, Edgemont, PA; 20X) equipped with a SPOT Insight QE camera (SPOT Diagnostic Instruments, Sterling Heights, MI) was used at 4X and 20X magnifications to visualize the crystals. Other samples were crushed using a ceramic mortar and pestle, and then spread onto a glass sample holder, sealed with thin Kapton film to prevent evaporation and characterized by X-ray diffraction (Rigaku MiniFlex II, Rigaku Americas Corp., The Woodlands, TX. Anode current 30 mA accelerating voltage 30 kV, scanning from $2\theta=5°$ to 40° with a step size of 0.02° using CuKα radiation).

4.4. Results and Discussion

a

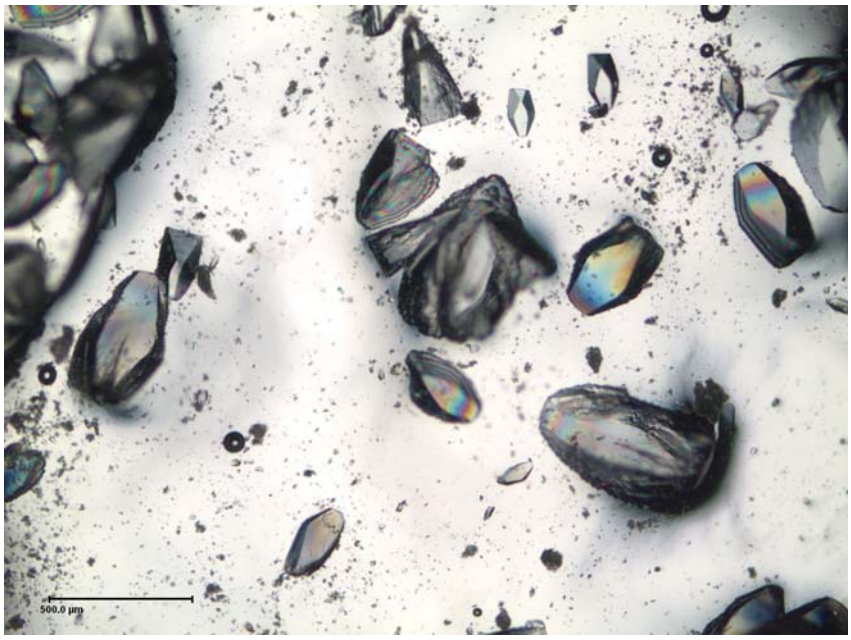

b

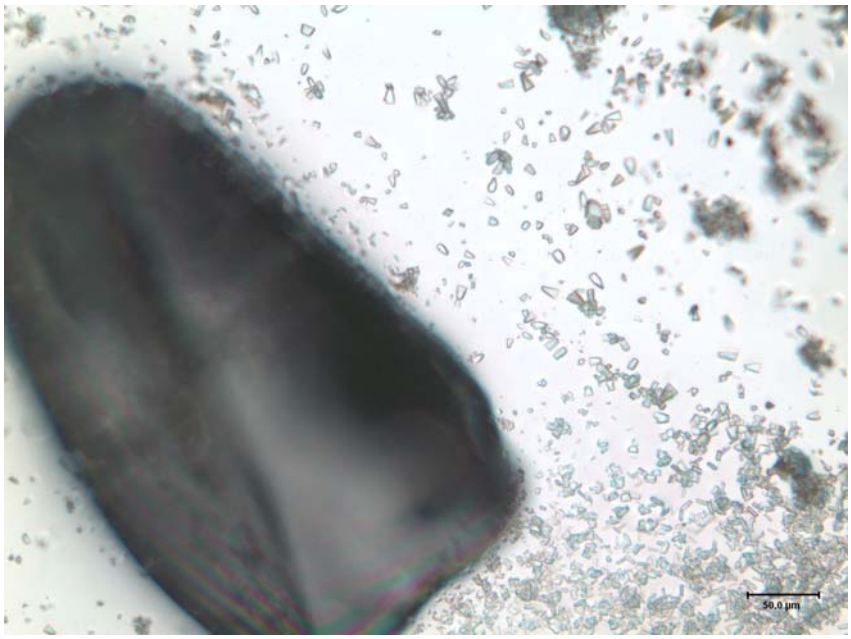

Figure 4.2. Micrographs of lactose crystals obtained from a gelatin-gel (43 wt% lactose, 1.5 wt% gelatin) after 24 hours at 25°C(a) 4X (scale bar = 500 µm) and (b) 20X (scale bar = 50 µm) magnifications.

After crystallizing for 24 hours, the crystal structure and morphology were characterized by optical microscopy (Fig. 4.2 a-b) and powder XRD (Fig. 4.3). A range of different crystal sizes and shapes were observed. Since the secondary nucleation was prevented within the gel environment, it can be assumed from the polydispersity in size that nucleation and crystal growth occurred simultaneously throughout the crystallization.

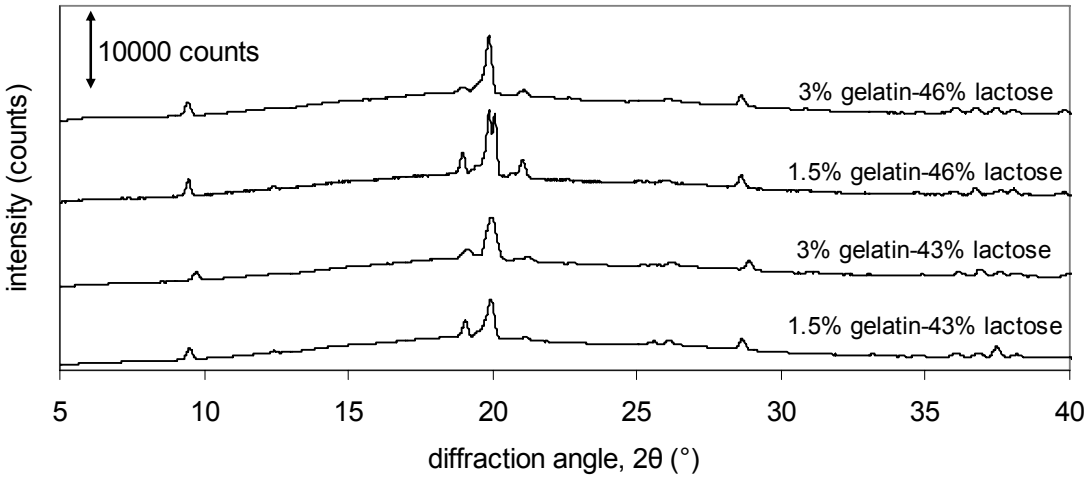

Figure 4.3. XRD patterns after 24 hour crystallization of gelled (1.5-3 wt% gelatin) lactose (43-46 wt%) solutions at 25°C.

The crystalline microstructure formed under different conditions was studied by XRD analysis (Fig. 4.3). All treatments produced peaks in similar positions but sometimes with differing magnitudes suggesting the crystals formed were similar to one another. I am not able to provide a complete analysis of the X-ray patterns from this level of information but, the peak at 20° corresponds to the major peak for α-lactose monohydrate (i.e., the stable crystal form typically obtained from aqueous solution) (Buma and Wiegers, 1967). However the other characteristic peaks of α-lactose monohydrate (12.5° and 16.4°) were not observed and the overall pattern was more similar to that of anhydrous α-lactose - typically formed after drying crystals at high temperatures - given by (Figura and Epple 1995). Haque and Roos, (2005) reported a similar XRD pattern for both α-lactose monohydrate and anhydrous mixtures of α- and β-lactose in a molar ratio of 5:3 obtained

from spray dried aqueous lactose-gelatin solutions, which gave the highest intensity peak at diffraction angle of 20°.

Gel system upon cooling:

The gelatin gelled quickly after cooling in the waterbath and was solid after 15 minutes Gelatin gels more rapidly and forms stronger gels in the presence of sugars (Kasapis et al. 2003). Similar samples prepared without lactose remained liquid for over an hour. The gelation of the gelatin component occurred more rapidly than the lactose crystallization so the lactose crystals were trapped in the gel and did not sediment. A photograph of crystallizing samples is given in Appendix B.1.

Ultrasonic measurements:

Ultrasonic and optical measurements were started 15 min after placing the sample into the water-bath to ensure thermal equilibration. Ultrasonic velocity increased with gelatin concentration (Fig. 4.4a) while the attenuation of the solutions (prior to lactose crystallization) was low and not affected by changes in gelatin concentration (Fig. 4.4b). Neither velocity nor attenuation was affected by gelation of the gelatin alone (data not shown).

a

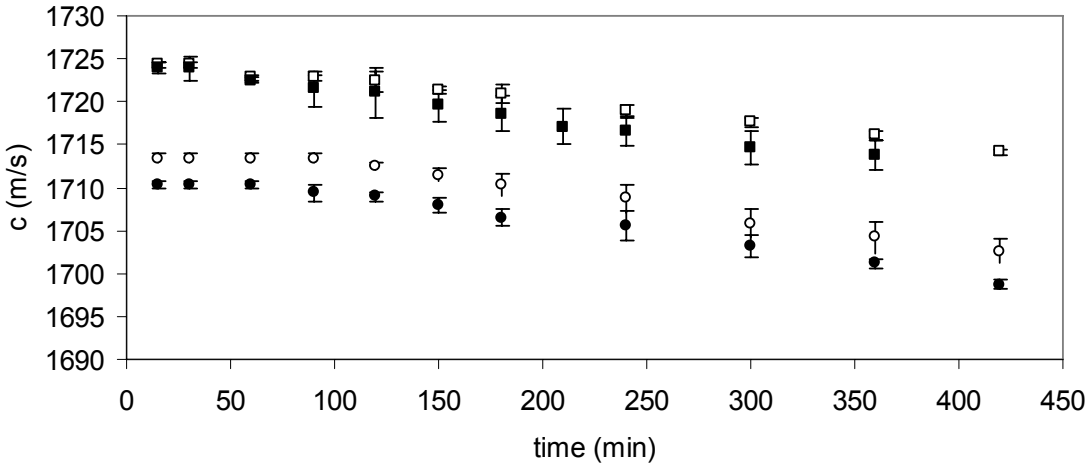

b

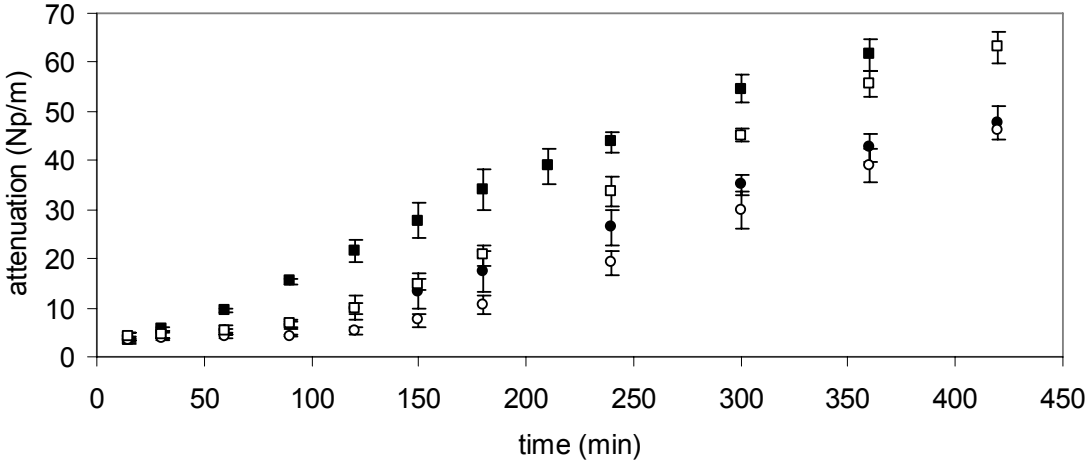

Figure 4.4. Ultrasonic (a) velocity and (b) attenuation measurements (2.25 MHz) on lactose crystallization at 25°C from aqueous solutions of (●) 1.5 wt% gelatin and 43 wt% lactose, (○) 3 wt% gelatin and 43 wt% lactose. (■) 1.5 wt% gelatin and 46 wt% lactose, (□) 3 wt% gelatin and 46 wt% lactose. Data shown are the mean and standard deviation of three separate experiments.

At the beginning of the experiments, when all the lactose was dissolved, ultrasonic velocity increased with lactose concentration (see also similar findings in Chapter 3). However, crystallization of the fine particles scatters the acoustic wave and lead to measurable changes in signal. Ultrasonic velocity decreased modestly (<10 ms^{-1}, ~0.5%) during the course of the experiment (Fig. 4.4a). Typically crystallization leads to an increase in velocity since the speed of sound is faster in solids than in liquids but in this case scattering effects dominate resulting in the slight decrease seen.

Ultrasonic attenuation increased substantially during the crystallization process for all samples but the kinetics were different for different formulations (Fig. 4.4b). The attenuation measurements were more sensitive to crystallization than velocity measurements, and thus provide a potentially better description of the process. At first glance it appears that crystallization was slower at higher gelatin concentrations and significantly faster at higher lactose concentrations. However ultrasonic attenuation in a dispersion is a function of particle size as well as particle concentration so attenuation cannot be taken directly as a measure of mass crystallization. Different formulations can change the relative rates of crystal nucleation and growth yielding to variations in number and size of the crystals for the same degree of crystallization. For example larger crystals observed with increasing gelatin concentration might have been modified the attenuation measurements to an unknown extent.

Optical measurements:

The initial absorbances of all samples were low and similar and increased with crystallization of lactose (Fig. 4.5). The kinetics of order of absorbance change was different with varying formulation and similar to behavior noted for ultrasonic attenuation measurements (Fig. 4.4b). The absorbance of the gelatin solution changed as the gel developed over several hours so it was necessary to use a gelatin-water blank in these experiments.

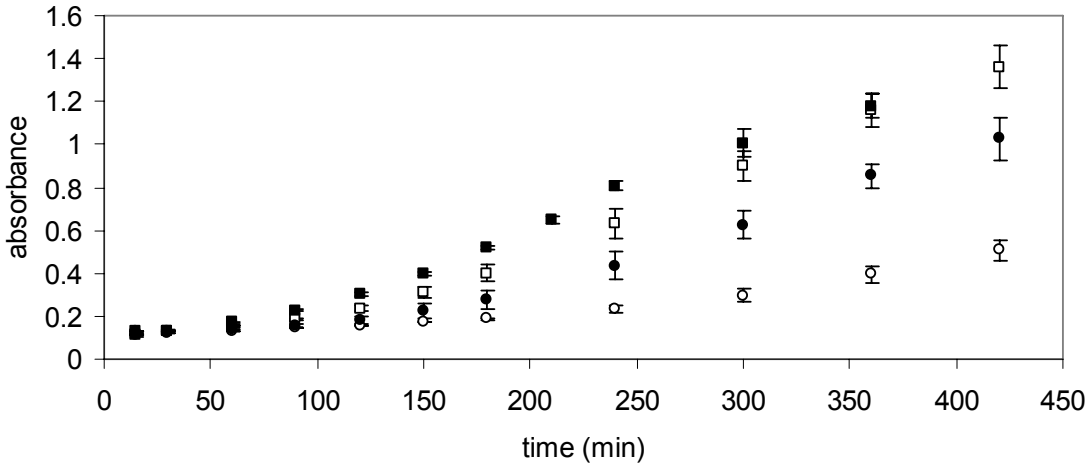

Figure 4.5. Corrected absorbance measurements (500 nm) of lactose crystallization at 25°C from aqueous solutions of (●) 1.5 wt% gelatin and 43 wt% lactose, (○) 3 wt% gelatin and 43 wt% lactose. (■) 1.5 wt% gelatin and 46 wt% lactose, (□) 3 wt% gelatin and 46 wt% lactose. Data shown are the mean and standard deviation of three separate measurements.

Rate parameters:

Two rate parameters were defined to compare the effects of formulation on lactose crystallization kinetics as measured by the various methods (Figure 4.6). First, the maximum rate of crystallization (r_{max}) was defined as the maximum rate of change in sensors' response. A linear regression was applied on three consecutive points where the maximum change per unit time was observed to calculate r_{max}. Secondly, the induction time (t_i) was calculated by extrapolating the maximum rate linear regression to the initial senor response value, as shown in Figure 4.6.

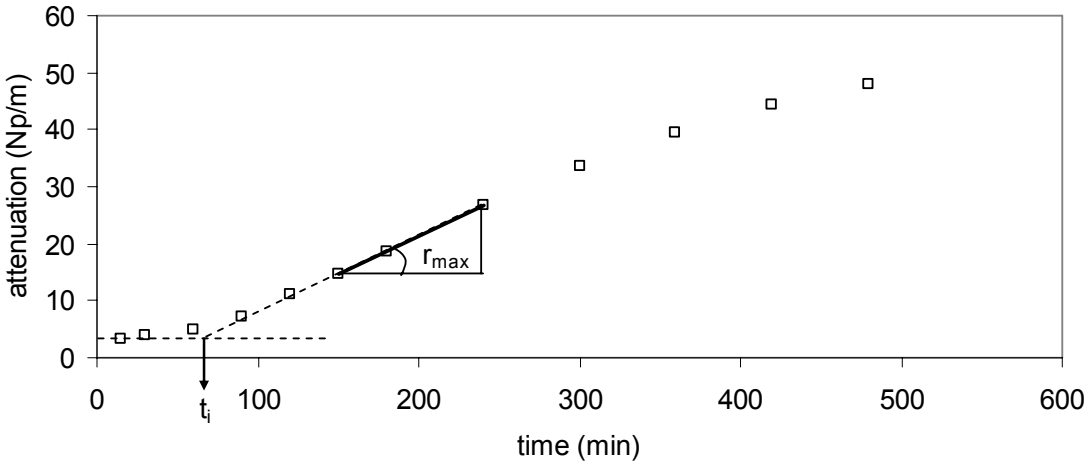

Figure 4.6. Calculation of kinetic parameters from ultrasonic attenuation measurements (2.25 MHz) on lactose crystallization at 25°C from the aqueous solution of 1.5 wt% gelatin and 43 wt% lactose. Solid line shows the linear regression (y = 0.133x – 5.255) drawn through the three data points where sensor response is changing most rapidly. The maximum rate (r_{max}) is taken as the slope of the line and the induction time (t_i) as the time when an extrapolation of the regression line equals the initial sensor value. A sample set of data is shown to illustrate calculations of the defined rate parameters.

The maximum crystallization rate was inferred from sensor response change and was not directly given as the degree of crystallization, because the calculation of percent crystallinity requires the complete information on the course of crystallization process. Since the presence of dispersed crystals have similar affect (i.e., scattering) on ultrasonic attenuation and optical absorbance measurements and optical measurements can not be used in opaque systems, my measurements were done until system loose its transparency. However, contrary to optical techniques, by manipulating intensity of the acoustic wave through pulser gain attenuation measurements could be conducted in optically opaque solutions (i.e., since they are mechanical waves and can travel in solids, this is a viable practice) to follow the complete course of crystallization. However, in this study crystallization process was investigated both by ultrasonic and optical methods until the samples became opaque.

Isothermal DSC:

The total course of the crystallization process was followed using isothermal DSC (Figure 4.7a-d). Rate parameters were calculated in a similar way to ultrasonic and optical measurements. However, in this case maximum crystallization rate was reported in terms of degree of crystallization (i.e., crystal change per unit time) since the crystallization process was followed to completion and heat released is proportional to the amount of lactose crystallized..

Comparison of different methods:

For all methods the maximum rate of crystallization increased with lactose supersaturation but was not significantly affected by gelatin concentration (Table 1, $p<0.05$). Because the sensor response was numerically different in each case the numerical values for the maximum rate varies between methods but is possible to compare and contrast the effects of formulation on the measurements. Although increasing gelatin concentration slowed the calculated maximum rate, the effect was not significant ($p<0.05$). The one exception to this rule was optical measurements where higher gelatin concentration significantly slowed the rate of crystallization in dilute lactose solutions. The reason might be due to the sensitivity of the turbidity measurements to simultaneous changes in the gelatin.

For all methods the induction time for crystallization decreased with lactose supersaturation but was not significantly affected by gelatin concentration (Table 1, $p<0.05$). Although induction times measured by acoustic and optical techniques are in the same order of magnitude, they are not exactly the same becuase they were calculated from the response of the different sensors which may respond differently to crystal size/number. The much higher induction time found for the DSC analysis could be attributed that all course of crystallization process was followed with this method, and total monitored crystallization period is noticeably higher than others.

a

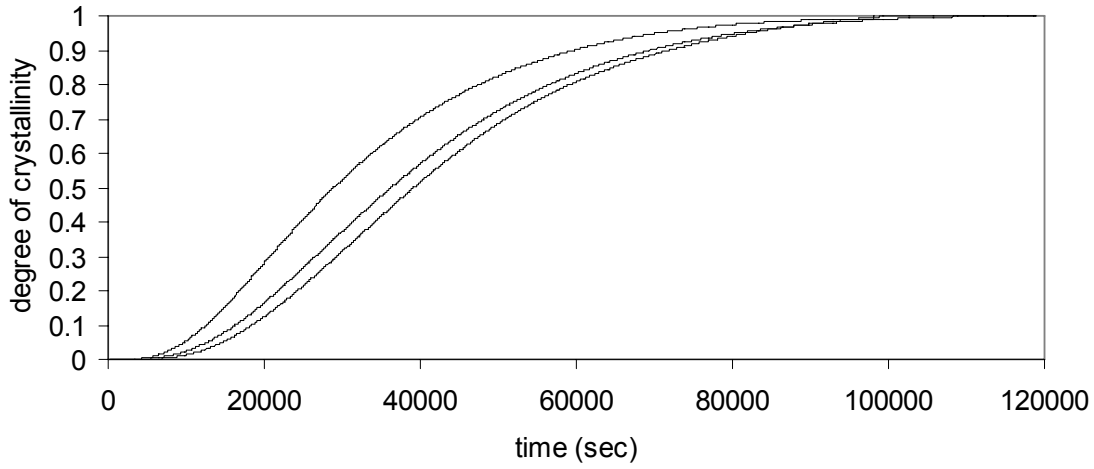

b

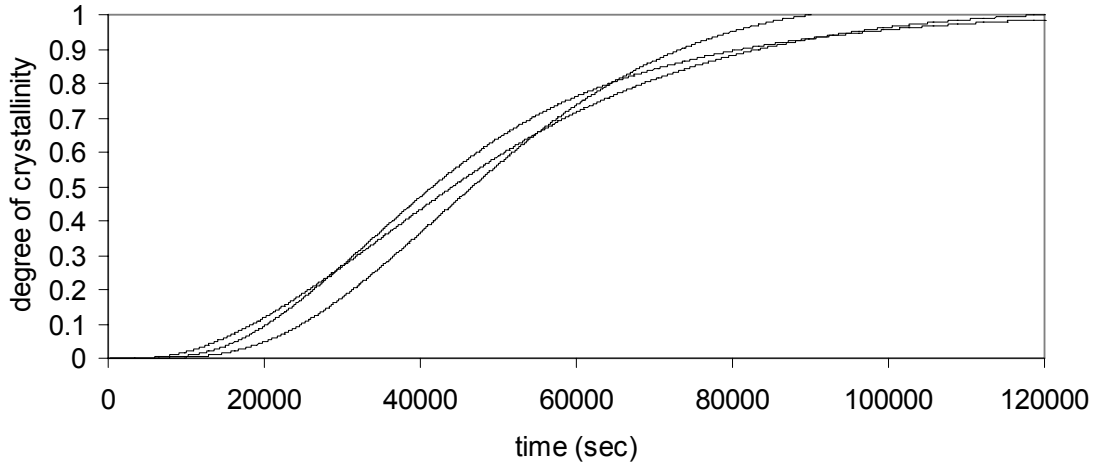

Figure 4.7. Lactose crystallization as calculated from isothermal DSC at 25°C for aqueous solutions of (a) 1.5 wt% gelatin and 43 wt% lactose, (b) 3 wt% gelatin and 43 wt% lactose. (c) 1.5 wt% gelatin and 46 wt% lactose, (d) 3 wt% gelatin and 46 wt% lactose. All 3 replications for each treatment were shown on the graph. (All graphs, a-d, are plotted together for comparison in Appendix B.3).

c

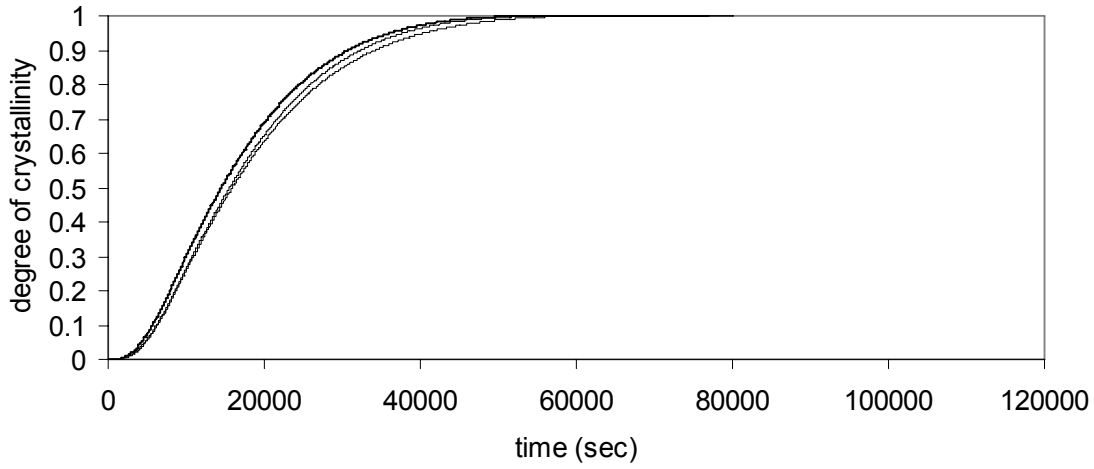

d

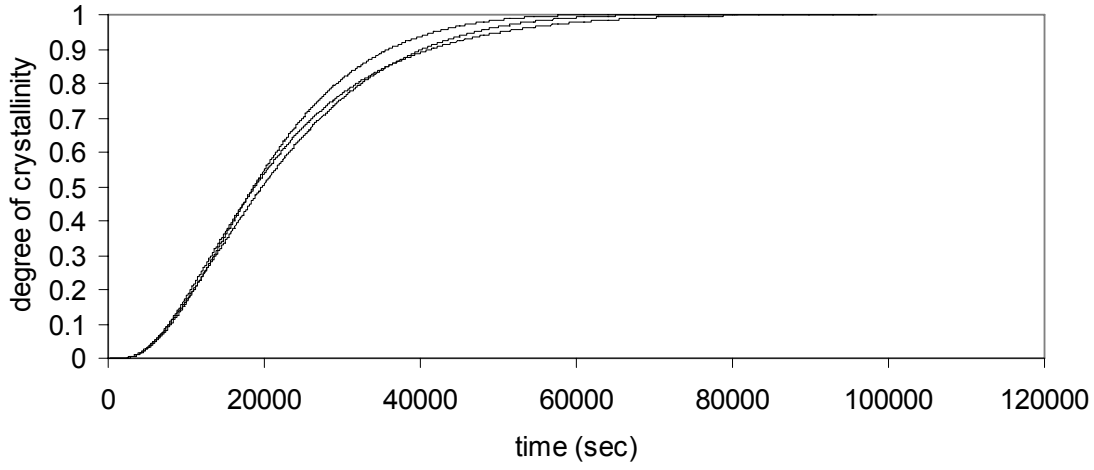

Figure 4.7. (Continued).

Induction time typically decreases and rate of crystallization increases with increased supersaturation (Hartel, 2001). For example, Raghavan et al. (2001) showed the induction time, induced by mixing, for lactose crystallization decreased from 8 h at 31°C (i.e., 70% supersaturation) to 2 h at 20°C (i.e., 130% supersaturation). The effects of gelatin on lactose crystallization are less well-studied.

From a review of the early literature, Whitaker (1933) concluded lactose crystallization can be delayed with gelatin, however large gelatin concentrations were required to be effective at high lactose concentrations. On the other hand, Nickerson (1962) showed that 0.4 wt% gelatin can delay lactose crystallization noticeably. However these works considered the lactose crystallization at refrigerated temperatures where the mutarotation can determine the crystallization rate, may not be possible to generalize their conclusions to higher temperature ranges. In a related work, Mimouni et al. (2005) showed that in the presence of whey proteins (~5 wt%) much smaller (~3 fold) lactose crystals were obtained as compared to protein-free solutions during non-seeded crystallization at 30°C, but overall crystallization rate constant was not affected. In contrast to the findings of the current work, Mimouni's study suggests the added protein reduces the lag time (because smaller crystals result from faster nucleation) and unchanged mass crystallization. However, Mimouni's work was with ungelled globular proteins which may interact via different mechanisms.

While in most cases gelatin had no significant effect on lactose crystallization kinetics, some significant differences were seen in the turbidity measurements. One reason for this may be because gelatin gelation led to changes in turbidity independent of changes due to lactose crystallization. Although this effect partially accounted for using the changes in pure gelatin solution as a blank, any interactions between gelatin and lactose molecules would not be calibrated out by this method. Alternatively both in ultrasound and optical methods the sensor response is affected by changing crystal size distribution and the size effects on long wavelength sound (~0.5 mm) may be different from short wavelength light (~500 nm).

Table 4.1. (a) Maximum rate (r_{max}) and (b) induction time (t_i) for sensor response and percent crystal content change (mean ± standard deviation, n=3). Different letters show significant difference ($p<0.05$) within a measurement method (i.e., acoustic, optical, or thermal).

(a) r_{max}

Composition	$r_{ultrasound}\times 10$ (α/min)	$r_{turbidity}\times 10^3$ (abs/min)	$r_{DSC}\times 10^5$ (%crystal/min)
1.5% gelatin, 43% lactose	1.65±0.20[a]	3.60±0.44[a]	2.26±0.30[a]
1.5% gelatin, 46% lactose	2.30±0.17[b]	5.03±0.12[b]	4.64±0.21[b]
3.0% gelatin, 43% lactose	1.61±0.12[a]	1.87±0.06[c]	1.87±0.18[a]
3.0% gelatin, 46% lactose	2.29±0.26[b]	4.37±0.25[b]	4.08±0.26[b]

(b) t_i

Composition	$t_{ultrasound}$ (sec)	$t_{turbidity}$ (sec)	t_{DSC} (sec)
1.5% gelatin, 43% lactose	107.2±27.8[ac]	161.0±21.5[a]	12097±2748[a]
1.5% gelatin, 46% lactose	51.6±11.4[b]	101.1±7.4[b]	4086±233[b]
3.0% gelatin, 43% lactose	144.0±12.8[c]	209.2±14.9[c]	16855±2925[a]
3.0% gelatin, 46% lactose	91.0±13.9[ab]	128.9±10.1[ab]	5546±491[b]

4.5. Conclusions

In this study, the applicability of *in-situ* ultrasonic measurements (2.25 MHz center frequency) to follow bulk crystallization of lactose (43-46 wt%) from gelatin gels (1.5-3 wt%) were investigated, and compared to turbidity (500 nm) and isothermal DSC measurements. Ultrasonic attenuation was found to be more sensitive to crystallization than ultrasonic velocity measurements. All measurement methods showed similar trends on lactose crystallization with changing formulation. In general, the rate of crystallization increased and induction time decreased with increasing super-saturation, and changing gelatin concentration did not show significant difference on kinetic parameters. Although the principles of both ultrasonic attenuation and optical absorbance measurements of crystal concentration in a dispersion are identical (i.e., both methods rely on the scattering of harmonic waves), ultrasonic measurements are preferred since they can be applied for opaque systems. Moreover, since ultrasonic measurements on crystal dispersions are strongly affected from changes in crystal size, spectral measurements can provide further information about crystal size as well as concentration.

Chapter 5

ULTRASONIC CHARACTERIZATION OF DISPERSIONS OF SUGAR IN VEGETABLE OIL

5.1. Abstract

Fine sugar crystals were dispersed into vegetable oil (8-16 wt%) in a stirred tank. The dispersed crystals were agglomerated by the addition of small volumes of water (<1%) and finally allowed to sediment quiescently. The process was monitored by continuous ultrasonic attenuation measurements.

Ultrasonic attenuation increased with increasing sucrose crystal concentration and degree of agglomeration. The agglomeration process was also found to be inhomogeneous as inferred from sedimentation kinetics and confirmed by micrometer measurements of crystal agglomerates. In conclusion, ultrasonic attenuation measurements can be used as a monitoring method to follow dispersing processes in food manufacturing, such as chocolate conching or flavor slurry preparation.

5.2. Introduction

Several food processing operations involve dispersing powders in liquids. During the mixing process, powder agglomerates are broken up and the viscosity of the suspension decreases. For example in chocolate conching, a long mixing process at elevated temperatures is necessary to disperse sugar, cocoa solids, and milk powder in liquid cocoa butter and convert the product from a paste to a smooth liquid (Beckett, 2009).

Particle dispersion involves three steps: wetting the surface with liquid (e.g., oil in conching) and displacing air, deagglomerating the wetted clumps, and finally maintaining particle separation and preventing sedimentation. Clearly, the strength and nature of the interparticle forces will determine the efficiency and effectiveness of the process. When hydrophilic particles are dispersed in a non-polar liquid any small amount of water present will adsorb at the particle surfaces and hold the powder in clumps by forming water bridges, i.e., strong capillary forces (Johansson and Bergenstahl, 1992a). This is particularly important in chocolate conching when a small amount for water can rapidly agglomerate the sucrose particles and increase the suspension viscosity. For example, Chevalley (1999) showed that the presence of 3-4% water increases the viscosity of molten chocolate markedly as compared to the typical moisture concentrations of 0.5-1.5%. Emulsifiers can assist the dispersion of fine particles by adsorbing at the surface and providing some steric repulsion (Johansson and Bergenstahl, 1992b).

The degree of agglomeration can be followed by measuring the particle size of the particles directly or inferred from apparent viscosity measurements (Beckett, 2001, 2009) or from sedimentation measurements (Johansson and Bergenstahl, 1992b). For studies of agglomerates formed by weak adhesion, sedimentation experiments are more suitable than rheological measurements as the forces applied to the aggregate during measurement are less (Johansson and Bergenstahl, 1995). Sediments formed from non-agglomerated particles tend to be more dense than sediments formed from agglomerated particles (Mongia and Ziegler, 2000). Moreover, sediment volumes of dispersions of sugar in oil

increased 50% with an increase in water concentration from 0 to 1%, (Johansson and Bergenstahl, 1992c).

Dispersions of crystals at concentrations and sizes commonly used in industry are often opaque, and so optical methods are unsuitable to study aggregation directly. However, ultrasound propagates well through most fluids and can be used to characterize dispersions. Acoustic waves move as a series of compressions and rarefactions in the material they are passing through. Wave propagation depends on the thermal and physical properties, such as density and elasticity, of the media so measurement of acoustic properties is related to material properties. Ultrasound is high frequency (i.e., >18 kHz) sound that at low power levels is non destructive and useful for sensing applications. Ultrasonic velocity and attenuation (i.e., the logarithmic loss of the wave energy with distance) can both be measured (Chanamai et al., 1998). However, attenuation measurements are often preferred for dispersion characterization, as it is less affected by small temperature changes (Povey, 1997).

Ultrasonic attenuation measurements have been used to measure the concentration (Bamberger and Greenwood 2004), size (Holmes et al., 1993) and degree of agglomeration (Bryant and McClements, 1999) of fine particle suspensions. Sedimentation kinetics can also be followed by measuring ultrasonic properties as a function of height and time during gravitational separation. This method has been applied to creaming measurements in emulsions (Pinfield et al., 1994; Basaran et al., 1998) including effects of flocculation (Chanamai et al., 2000). Previously, I demonstrated the use of ultrasonic attenuation measurements to follow the mixing kinetics of lactose crystals into a saturated lactose solution (Chapter 3). There was a large increase in attenuation of the sample immediately upon addition of the powdered lactose, which decreased during mixing to a steady state value dependent on the solids loading.

The objective of this study is to demonstrate the use ultrasonic attenuation measurements for on-line monitoring of mixing of sucrose crystals into oil and the agglomeration

process caused by the addition of water. The subsequent sedimentation kinetics determined by the degree of agglomeration is also to be followed by measuring the changes in ultrasonic attenuation due to composition change at a certain height. This model system study has parallels to the processes involved in chocolate conching and to the simpler process of favor slurry manufacture.

5.3. Materials and methods

Materials. Corn oil and confectioner's sugar (sucrose) were bought from a local market. Sugar was stored in a desiccator with Drierite until used. The crystals were characterized at room temperature by optical microscopy (Olympus BX-41, Hitech Instruments, Edgemont, PA; 20X) equipped with a SPOT Insight QE camera (SPOT Diagnostic Instruments, Sterling Heights, MI), static light scattering (Horiba LA-920, Irvine, CA assuming a relative refractive index of 1.12), and x-ray diffraction (Rigaku MiniFlex II, Rigaku Americas Corp., The Woodlands, TX). Sugar crystals were dispersed in isopropanol (≥99.5%, Sigma-Aldrich) prior to the optical analyses.

Mixing. The previously described stirred tank system fitted with ultrasonic sensors was used for mixing and sedimentation experiments (Chapter 3). A known amount of corn oil was introduced into the container (a cylinder with an internal diameter of 10.4 cm) and agitated with a blade impeller (5 cm diameter and 1.3 cm width with 0.6 cm diameter shaft) located at a position as in the middle of the total sample height and driven at 600-650 rpm by a laboratory scale stirrer (STIR PAK laboratory stirrer, Model 4554, Cole Parmer, Chicago, IL). Dry sugar crystals (8-16 wt%) were quickly added (i.e., in less than 30 sec) , and after the crystals were uniformly dispersed within the oil (i.e., no change in the mean sensor response with time), water was added to induce crystal agglomeration. In some experiments, the stirrer was stopped after the desired mixing was attained and subsequent sedimentation kinetics were followed ultrasonically.

All experiments were conducted at room temperature. Sample temperature, as monitored with a k-type thermocouple (0.1°C sensitivity), fluctuated around 22.8°C with a maximum deviation of 0.4°C. All experiments were performed at least in triplicate.

Ultrasound. The course of mixing process was followed on-line by ultrasonic attenuation measurements as described in detail in Chapter 3 and summarized as follows. A controlled electrical signal was generated and collected by a square wave pulser/receiver (Panametrics 5077 PR, Waltham, MA) and subsequently digitized by an oscilloscope (LeCroy 9310c, Chestnut Ridge, NY). Ultrasonic transducers (2.25 MHz center frequency) were located at 2/3rd of the total sample height from the sample surface in through-transmission mode. Attenuation data was collected automatically by a Lab View (version 7.1, National Instruments, Austin, TX) virtual instrument. The pulse gain was increased 03 dB for each 2 wt% increase in sugar concentration to ensure an acquirable acoustic signal was transmitted between the transducers. The energy of the incident pulse at each gain was calibrated with respect to the water. However at gains higher than 00 dB the transmitted wave energy in water was off scale for the oscilloscope, in which case they were extrapolated from measurements at lower gain values (See Appendix C.1). The energy loss within the sample was evaluated as a normalized power transmission loss (NPTL, Chapter 3):

$$NPTL = 10 \log (I_{water} / I_{measured}) \qquad (5.1)$$

where I_{water} and $I_{measured}$ are the intensities measured in water and the sample, respectively.

Solid bed density and solid bed height. The packing properties of the dispersed particles can be used as an indication of the degree of the agglomeration. After the desired mixing was attained, dispersions were characterized by means of solid bed density (SBD) and solid bed height measurements. Aliquots (~7 mL) of the dispersion was sampled into a 10 mL glass tube (1 cm diameter), and allowed to settle out over 48 hours. The sediment was characterized as the ratio of sediment volume to total volume, i.e., normalized solid bed

height (NSBH). The SBD was also calculated as described by Mongia and Ziegler (2000), i.e., the ratio of the total mass of the solids to the volume of the sediment.

5.4. Results and Discussion

5.4.1. Characterization of crystals

The particle size analysis by light scattering, showed a wide distribution of crystals with a volume-weighed average diameter ($d_{4,3}$) of 29.8±1.6 μm (Figure 5.1a). A micrograph (Figure 5.1b) of the sugar crystals is complementary to light scattering analysis and also shows a wide crystal size distribution and particles with irregular morphologies. The XRD pattern of the powdered sugar (Appendix C.2), was same with that of pure crystalline sucrose (Labuza and Labuza, 2004), with negligible diffuse background.

a

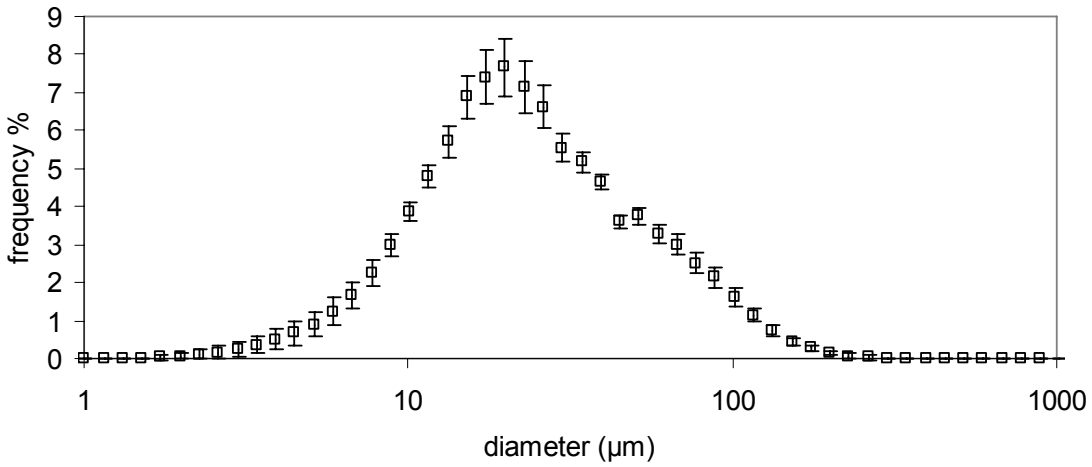

b

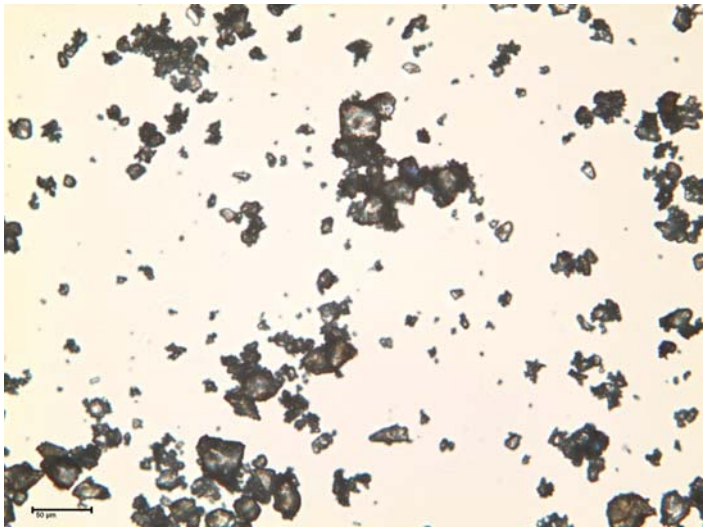

Figure 5.1. (a) Particle size distribution of sucrose crystals used as measured by light scattering (data point shown are the mean and standard deviation of 5 experimental replications) and (b) micrograph (scale bar 50 μm) of similar crystals used.

5.4.2. Dispersing the sugar crystals into oil

The changes in ultrasonic signal on adding sucrose to water are illustrated in Figure 5.2. The initial NPTL is not zero because pure oil dissipates more ultrasonic energy than water; however, as soon as the powdered dry sugar was added into oil (1 min) there is a sudden increase. The NPTL then decays back to a steady state value over about 2000 sec. Although only data from a single experiment is shown, the process is highly reproducible as all mixing profiles for the same composition effectively overlaid one another.

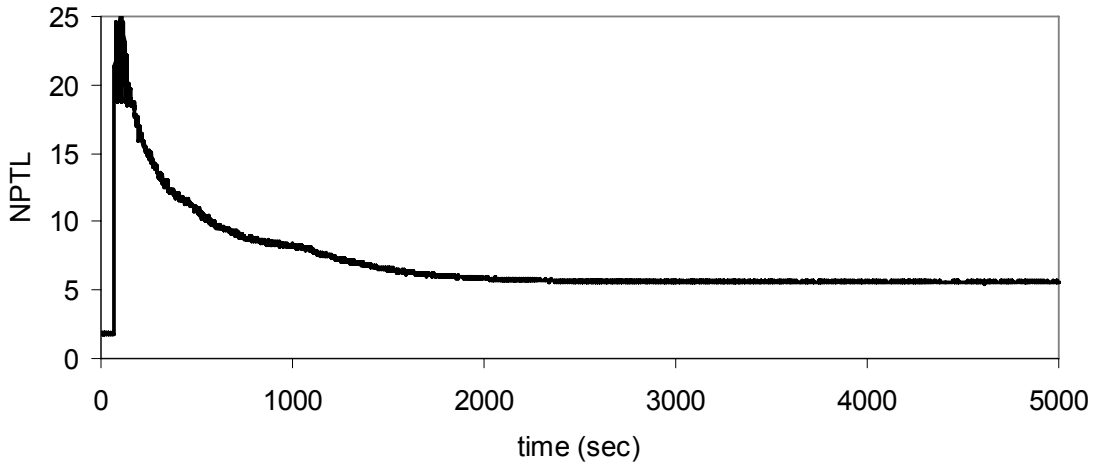

Figure 5.2. Kinetic changes in NPTL upon addition of 80 g sucrose crystals into 920 g corn oil (i.e., 8 wt% dispersion). The sucrose was added at 60 seconds and the total addition time was less than 30 sec. Measurements were made every 0.5 sec. and the line shown is a moving average over three points.

When solid powder is added into a liquid, it first distributes itself as clusters of particles with air pockets between and around them. As the mixing continues, the surfaces of individual particles are wetted with oil, the particle clusters are broken down and air is released. Entrained air bubbles can attenuate sound very strongly (Chapter 3), and I expect that changes in air content is mainly responsible for the changes seen in Figure 5.2, although change in effective particle size due to deagglomeration may play some role.

In this case, the plateau in the NPTL (i.e., steady state mixing) was reached after about 2000 sec. However, when lactose was added into a saturated lactose solution the steady state plateau was reached in only 120 sec (Chapter 3). This difference may be because sugars are hydrophilic in nature, and thus surface wetting is expected to be faster by water than hydrophobic oil molecules. Another possible mechanism may be related to the presence of any residual water in the lipid-continuous system, which can support the agglomerates by strong capillary forces.

Equilibrium NPTL (i.e., the steady state value from Figure 5.2) increased approximately linearly with sugar concentration (Figure 5.3), as is typical for dispersions provided their microstructure remains reasonably constant with changing concentration (Challis et al., 2005). In this case, NSBH also increased approximately linearly with sugar concentration (Figure 5.4) suggesting that the SBD, i.e., the way the particles pack together is unchanged (~0.47 kg sugar / m^3 sugar). Note that in both cases the linear relationship with sugar concentration began to break down at the highest concentration selected (16 wt%).

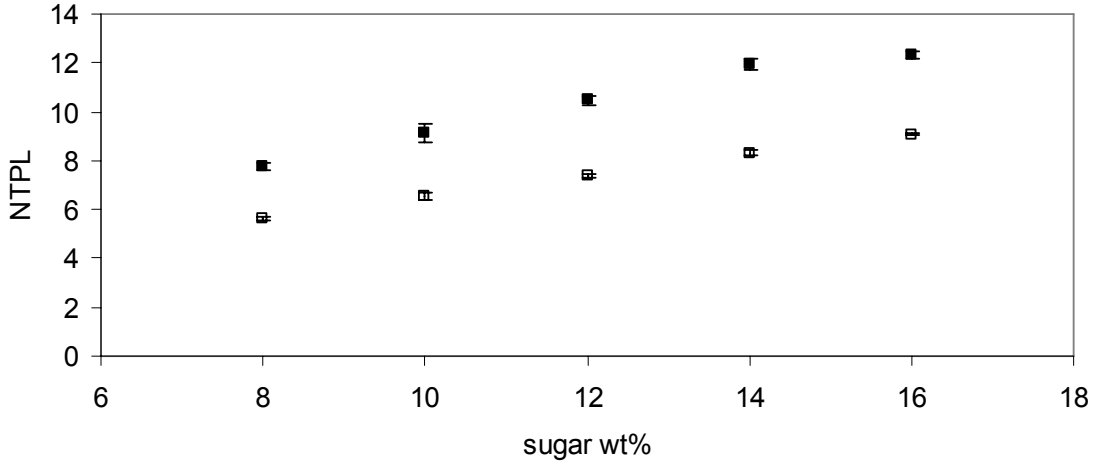

Figure 5.3. Steady state and quasi steady state (i.e, 3000 sec after water addition) NPTL for sucrose dispersions in corn oil containing (□) 0 and (■) 1% water (vol. water/wt. sugar) with respect to sugar content, respectively. Points and error bars are the mean and

standard deviation of three experimental replications. In each experimental run the plateau value was calculated as the average of 300 measurements made over 150 sec.

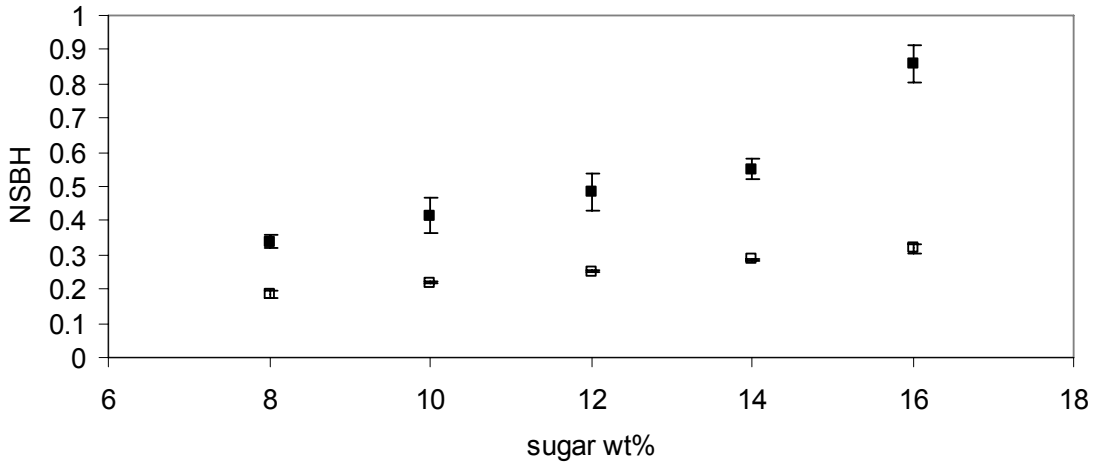

Figure 5.4. NSBH of sugar in corn oil dispersions containing with respect to sucrose content. Points and error bars are the mean and standard deviation of six experimental replications.

5.4.3. Addition of water:

After the sugar was fully dispersed into corn oil (i.e., steady state NPTL response in Figure 5.2), 1% (vol. water/wt. sugar) was added into the dispersion (Figure 5.5a). After a small lag time (30 sec) following the instantaneous water addition, NPTL increased rapidly over about 300 sec to a new plateau value (Figure 5.5b). In fact, the plateau continued slowly but significantly to increase with time (slope 2.1×10^{-4} s^{-1}, $p<0.05$). However, this slope was not considered important to the present work and the data were truncated at 3000 sec which was defined as a quasi steady state in the presence of water. The noise in the ultrasonic signal was much greater after the addition of water.

When water is present, it partitions onto the surface of the hydrophilic sugar crystals and holds them together as aggregates via strong capillary forces. The change in particle microstructures leads to the change in NPTL observed.

Addition of water also led to an increase in the sediment volume because aggregated particles pack together less efficiently (Appendix C.3). The SBD was about 0.25 (kg sugar / m^3 sugar) for all samples containing added water (except 16%) suggesting the structure of the aggregates was governed by the amount of water added rather than the amount of sucrose present (ANOVA analysis, $p<0.05$). However, changing the amount of water added while holding the sucrose concentration constant led to a progressive increase in bed height suggesting the aggregates were larger (Table 5.1). My findings are similar to those of Johansson and Bergenstahl (1992c) who showed that the volume of a sucrose crystals (largest particle dimension of 30 μm) sediment in refined soybean oil increased 50% when the moisture content increased from 0 to 1%.

Both NPTL and NSBH the 16% samples did not exactly follow the linear dependence on sucrose concentration seen with the more dilute samples. The deviation from linearity was greater in the presence of water than in the water-free samples.

a

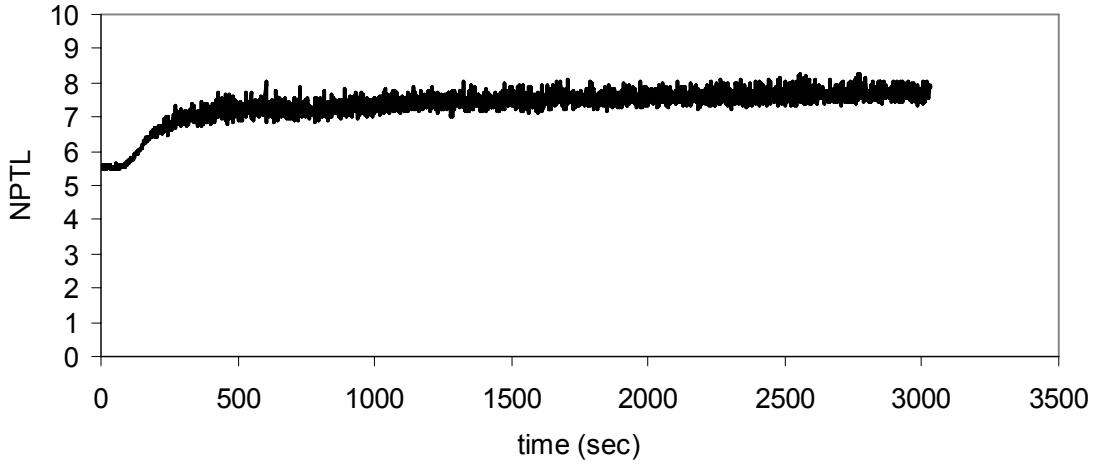

b

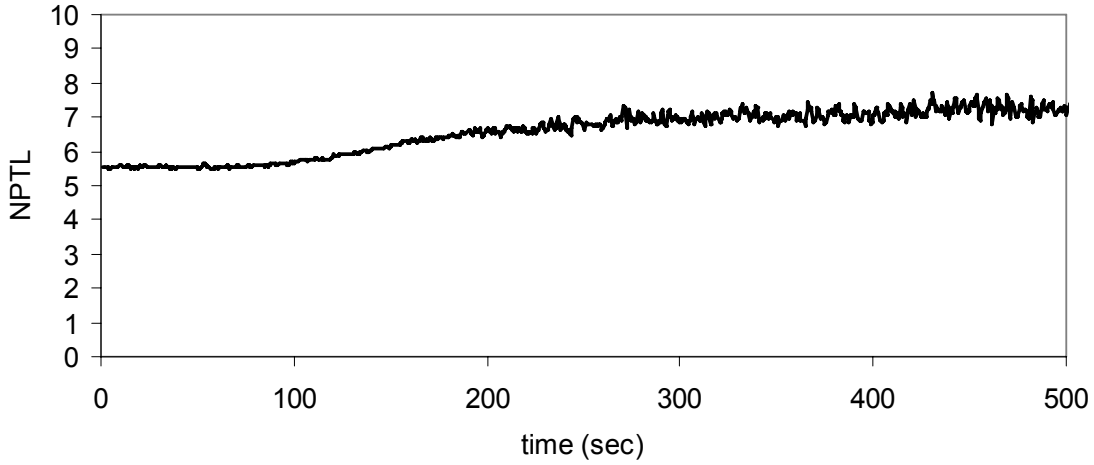

Figure 5.5. (a) Kinetic changes in NPTL upon addition of 1% water (vol. water/wt. sucrose) into 8 wt% sucrose dispersions in corn oil (i.e., 0.8 mL into the dispersion of 80 g sugar in 920 g corn oil), with (b) a zoom for the first 500 sec. Water was added after 50 sec. after the start of the experiment. Measurements were made every 0.5 sec. and the line shown is a moving average over three points.

5.4.4. Sedimentation

After the dispersions had reached steady state (i.e., in the case of dry dispersions) or quasi steady state (i.e., for the water added samples), the mixing was stopped and the particles were allowed to sediment out under gravity. During sedimentation, changes in composition in a fixed cross-section through the sample (i.e., acoustic beam path) were followed by NPTL measurements (Figure 5.6).

In the water-free samples (Figure 5.6a), there was no change in NPTL for about 18000 sec after mixing stopped, and then the signal briefly increased followed by a decrease to a NPTL value equal to that of sugar-free oil. Presumably, during the lag period, the sedimenting particles entering to the top of the ultrasonic beam path volume from above matched by those leaving from the bottom and the signal was unchanged. The increase in NPTL after the lag must be due to an accumulation of particles in the beam path as the rate of sedimentation at the bottom of the beam path is less than the rate of sedimentation at the top. Sedimentation rate tends to decrease as volume fraction increases (Darby, 2001) so the accumulation of particles near the bottom of the tank may serve to slow the movement of particles lower down more than the ones higher up. Alternatively the difference in the settling rates of small vs. large particles may contribute to the change in signal seen. The final decrease in NPTL to a steady state value corresponding to sugar-free oil is obviously due to the sedimentation of all of the sucrose particles to below the beam path. A similar concentration change was noted for a creaming emulsion by Pinfield et al. (1994), who simulated the changes in spatial distribution of colloidal size emulsion droplets upon storage by ultrasonic measurements.

a

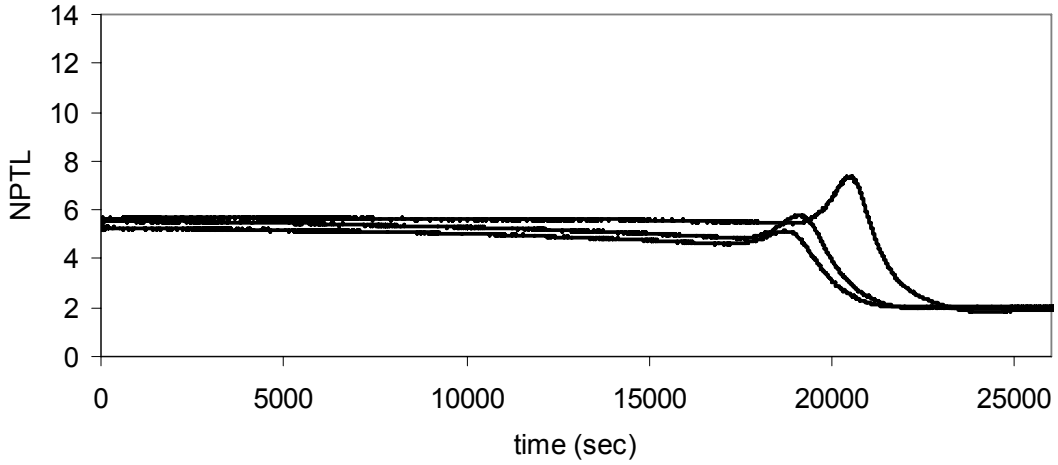

b

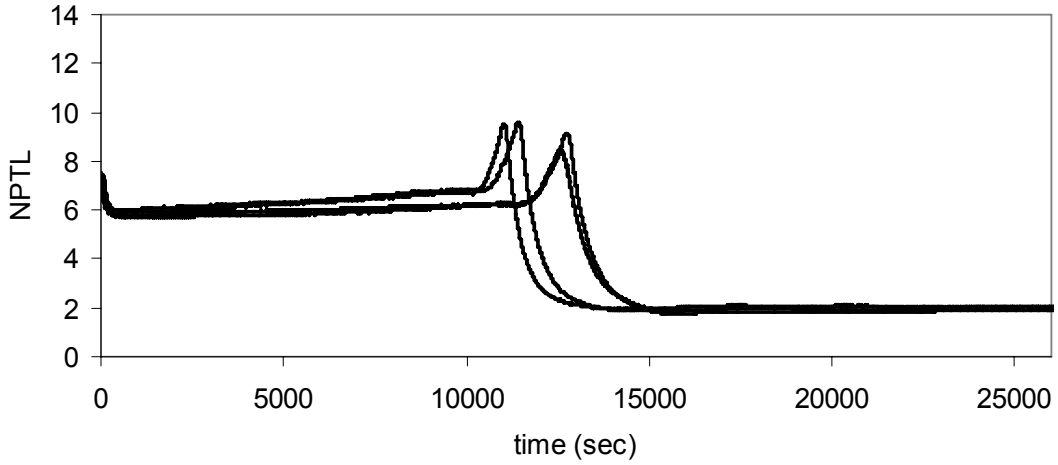

Figure 5.6. NPTL change due to sedimentation of sucrose particles in corn oil (8 wt%) with water contents of (a) 0, (b) 0.5, and (c) 1% (vol. water/wt. sugar). Measurements were made every 0.5 sec. and the line shown is a moving average over three points. Data from three or four replicate experiments are shown on each plot.

c

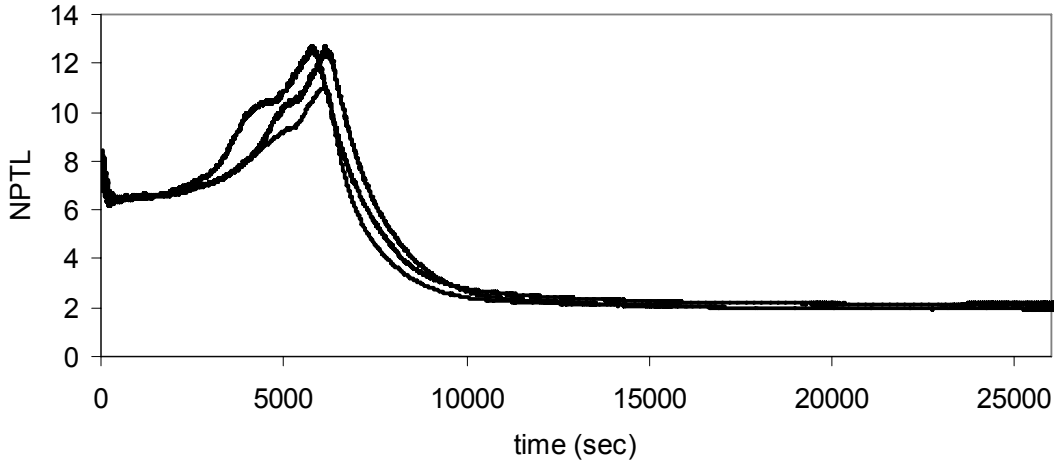

Figure 5.6. (Continued).

The sedimentation profiles of samples containing water (Figures 5.6b and c) were similar to those of the water-free samples with two important differences. First, the time lag before changes were seen decreased with increasing water content; and second, there was an immediate drop in NPTL in the first few minutes after the mixing was stopped. Adding water led to particle aggregation (see NSBH data for these samples in Table 1) and large particles sediment more quickly. Increasing the water content from 0 to 1% decreases the sedimentation time (taken as the time to reach the steady state plateau) from about 23000 sec to 10000 sec. Assuming the particles movement is governed by Stokes law this would correspond to about a $\sqrt{2}$ increase in effective particle size on water addition assuming the agglomerates were uniform. However, the very rapid initial decrease in NPTL was probably due to the formation of a few very large aggregates which sedimented much more quickly. When the samples were analyzed with a micrometer (i.e., sensitive to the largest particles present), particles in the water-free samples were too small to be detected (i.e., < 0.1 mm) while the some of the particles at the bottom of the sediment bed in the water-added samples were in the order of 1.5 mm. The fact that the water-added samples were much more heterogeneous than the water-free

samples goes some way to explaining the increased noise in the NPTL signal after adding water (Figure 5.5).

Table.5.1. Normalized solid bed height (NSBH) for 8 wt% sugar in oil dispersion (i.e., 80 g sugar, 920 g oil) as a function of amount of water added. Data are shown as mean ± standard deviation (n=6) and values marked with different letters were significantly different from one another ($p<0.05$).

% water (vol. water/wt. sugar)	NSBH
0	0.184 ± 0.022^{a}
0.5	0.273 ± 0.018^{b}
1	0.340 ± 0.019^{c}

Conclusions

The aim of this study was to demonstrate the applicability of ultrasonic attenuation measurements to monitor the process of dispersing sugar crystals in oil directly and continuously. It was also shown that ultrasonic measurements are sensitive to the agglomeration state of the crystals, which was changed by controlling the water concentration in the system, as confirmed by solid bed volume analyses. Subsequent sedimentation kinetics was followed with the same technique as concentration changes in a specified dispersion volume, providing further information on the agglomeration state of the dispersed particles. Consequently, ultrasonic attenuation measurement technique was presented as a candidate to monitor mixing processes, often a concern in food industry (e.g., chocolate conching, flavor slurry preparation).

Chapter 6

CONCLUSIONS AND RECOMMENDATIONS FOR FUTURE WORK

Ultrasonic waves are sensitive to the bulk properties (i.e., density and compressibility) of a homogenous system (e.g., solution), and are often modified by the characteristics of the different phases in a dispersion. Since ultrasonic measurements are rapid (i.e., suitable to follow kinetic changes with resolutions of less than seconds) and can be used on-line without disturbing the process or affecting the sample properties, they can help in improving the efficiency of industrial processes.

The aim of this study was to investigate the applicability of ultrasonic techniques to the characterization of crystal dispersions. The primary focus of this study was on the practical aspects of the use of ultrasonic techniques as sensors rather than on modeling the sound-matter interactions at a microscopic level. The target systems were the dispersions of crystals of small molecule sugars of varying particle sizes including large particles, i.e., with dimensions outside the long-wavelength limit. The particles were dispersed in different liquid continuous phases, i.e., with different hydrophobicities, to change dispersion properties. Steady state properties, as well as kinetic changes, in the dispersions were analyzed using ultrasonic attenuation and velocity measurements. The accomplished goals, as well as outstanding questions are summarized as follows.

On the measurement technique(s):

The experiments were done in two configurations: in an analytical scale high precision measurement cell, i.e., a pulse-echo reflectometer, and a larger scale stirred tank using through-transmission ultrasonic measurements. In both cases, the results were reproducible and similar results were obtained regardless of the configuration. All ultrasonic measurements were done using a narrow band ultrasonic transducer at a single center frequency (2.25 MHz center frequency). However, more detailed information about the dispersion properties, such as particle size distribution, can be obtained using a range of ultrasonic frequencies.

The first goal:

The first goal of this study was to evaluate the applicability of ultrasonic measurements to measure the compositions of lactose-water mixtures (i.e., solution or dispersion) at steady state. It was shown that the ultrasonic velocity is linearly related with dissolved lactose concentration in solution, and changing with crystal content depending on the properties of the dispersed phase. For example, in Chapter 3 it was found that velocity increased linearly with total lactose concentration (0-40 wt%) regardless of the state of lactose molecules, i.e., either dissolved or crystals. In Chapter 4 there were some changes in velocity during crystallization but these were relatively small (<0.5%) and not useful for characterizing of the process. In contrast to the ultrasonic velocity measurements, ultrasonic attenuation was relatively unaffected by changes of lactose concentration in solution, but increased with dispersed crystal amount. Similarly attenuation was low in oil and increased with dispersed sucrose crystal concentration (Chapter 5). Furthermore, aggregation of sucrose crystals in oil (induced by adding water) increased ultrasonic attenuation.

One application of these findings is to investigate changes in local concentrations of dispersed crystals during a mixing process. An array of ultrasonic transducers positioned at different heights, or a pair of transducers moving along the height, of a stirred tank may give information about the mixing profile and concentration distribution throughout system. One outstanding question from this part of the work is the behavior of acoustic waves in real foods, especially confectionery products. For example, ultrasonic techniques can potentially be used to monitor chocolate tempering on-line, if they are sensitive to changes in (re)crystallization of cocoa butter in the complex environment of chocolate paste (i.e., a matrix of cocoa butter, sugar, milk solids, and probably emulsifiers and some water.

The second goal:

The second goal was to follow the kinetic processes of dissolution (Chapter 3) and crystallization (Chapter 4) for the lactose-water systems. Since ultrasonic attenuation is more sensitive to the presence of dispersed particles in a liquid than velocity

measurements, continuous automated attenuation measurements were made during these processes.

Dissolution (Chapter 3):

The dissolution of lactose crystals and consequent changes in the system properties were monitored in the stirred tank configuration continuously and non-invasively by ultrasonic attenuation measurements and compared to off-line refractive index measurements. The rate of dissolution was controlled by varying the degree of under-saturation.

When lactose crystals (d~50 μm) were added into water or an under-saturated lactose solution, two processes took place consecutively. First the crystal surfaces are wetted with water molecules, and then the lactose dissolves. However, surface wetting is not instantaneous but limited by the deagglomeration rate of solid particles, and by the removal of air between the particle clusters. The air pockets present between and around the particle clusters attenuated the sound and introduced a dead time (i.e., a period that the changes due to dissolution were masked by the strong attenuation of air) to the measurements. In order to reduce the amount of air incorporation, and so the associated dead time, the dissolution process of α-lactose monohydrate crystals was achieved by adding water to mixtures of saturated lactose solution and crystals at equilibrium yielding an under-saturated solution at the end. Hence the subsequent dissolution process was monitored continuously and on-line from ultrasonic attenuation measurements. The calculated dissolution rate constant (~700 μs^{-1}) at 37°C was in agreement with literature data.

It may be possible to extent this method to obtain simultaneous particle size distribution and concentration data via spectral measurements and an appropriate theoretical model. However, particle size determination using the existing theories (e.g., ECAH theory) requires accurate and well defined physical and thermal properties of the components of a dispersion and is also limited to small size particles (i.e., in the long wavelength limit). One empirical alternative would be to use, pre-prepared calibration charts to calculate particle size distribution from ultrasonic measurements.

Crystallization (Chapter 4):

The bulk crystallization of lactose from gelatin gels was also monitored by ultrasonic attenuation measurements using a modified pulse-echo reflectometer as an immersion probe and compared to turbidity measurements. Isothermal DSC provided useful information on crystallization kinetics by measuring the enthalpy of crystallization. Induction time and crystallization rates were compared for varying degrees of super-saturation (43-46 wt%) and gelatin (1.5-3.0 wt%) concentrations.

The gel environment allowed homogenous distribution of crystals and hindered the convection flow effects and secondary nucleation. The crystallization rate of lactose increased with increasing degree of supersaturation, but was not affected by changing gelatin concentration. Although all measurements able to differentiate changes in crystallization behavior with changing system composition, ultrasonic measurements are preferred as on-line monitoring tools over turbidity measurements, which were affected by the changes in turbidity due to gelatin gelation and cannot be used when the dispersion becomes opaque due to lactose crystallization.

In the present work, lactose and gelatin concentrations were chosen arbitrarily to provide a range of suitable crystallization kinetics to assess the ultrasonic sensor. However, having established ultrasonics as an appropriate methodology, attenuation measurements could be applied more thoroughly to study the phase behavior of water-lactose-gelatin system, including optically opaque formulations. Moreover, a more detailed knowledge on the effects of lactose-gelatin interactions on lactose crystallization, as well as crystal morphology, could be obtained from ultrasonic measurements utilizing an appropriate experimental design.

The third goal (Chapter 5):

The third goal of this study was concerned with a model for the conching process in chocolate manufacture (i.e., dispersions of sucrose crystals in a vegetable oil) (Chapter 5). The dispersion process, i.e., deagglomeration of powdered sugar, was monitored in the stirred tank configuration using continuous ultrasonic attenuation measurements. The

degree of agglomeration was also varied by varying water concentrations and confirmed with solid bed volume measurements. Furthermore, subsequent sedimentation kinetics were continuously monitored using the same technique.

In a similar manner to the observations in dissolution section, the sudden increase in absorbance due to air incorporation upon addition of powdered sugar and subsequent decrease with deagglomeration of particle clusters (i.e., dead time in the dissolution analysis) was used to follow the course of dispersing process. It was found that the deagglomeration of sugar crystals in oil was much slower than in an aqueous environment (Chapter 3) due to the hydrophobic nature of the oil. Additionally, it was shown that the ultrasonic attenuation measurements were sensitive to the degree of agglomeration, *per se*. When small amounts of water ($\leq 1\%$) were added into the dispersion, it partitioned onto the surface of the hydrophilic sugar crystals and held them together as aggregates via strong capillary forces. The degree of agglomeration was characterized as an increase in the sediment volume because the aggregated particles pack together less efficiently. The subsequent sedimentation kinetics, as followed at a certain height from the bottom of the container through the ultrasonic beam path, was used to provide further information about on the state of agglomerated sucrose crystals. The sedimentation rates increased with degree of agglomeration (e.g., the total sedimentation time decreased to half of by 1% water addition) as expected. Moreover, it was found that the agglomeration process was inhomogeneous as confirmed by micrometer measurements and resulted in uneven sedimentation profiles.

This approach provides an interesting and novel approach to the characterization of sugar dispersions in oil which could be explored in a variety of ways. First, the degree of agglomeration can affect the apparent viscosity of the dispersion. If viscosity was measured independently, it may be possible to correlate non-invasive, on-line ultrasonic measurements with invasive, off-line rheological measurements. Controlling the rheology of some products during food processes, such as chocolate conching or flavor slurry preparations, is vital as it determines the final product quality. On-line ultrasonic

measurements can provide direct control over the rheology of the dispersion and thus over- (or under-) processing can be minimized.

Mechanistic models developed from equations of fluid dynamics could be used to simulate the sedimentation kinetics and check the validity of ultrasonic measurements. Separation processes, such as sedimentation (i.e., a gravitational separation), are a widely used in food industry, especially in refining operations. By on-line monitoring of the sedimentation kinetics, which is often difficult due to the opaque nature of the material, the factors (e.g., particle size distribution, and physicochemical properties of the respective phases) affecting the kinetics of this process could be better understood. Moreover, these measurements integrated with mechanistic models can also provide information about the stability of dispersions to the gravitational force.

REFERENCES

Akulichev VA, Bulanov VA (1981). Sound propagation in a crystallizing liquid. Soviet Physics-Acoustics, 27 (5), 377-381.

Akulichev VA, Bulanov VA (1983). Crystallization nuclei in liquid in s sound field. International Journal of Heat and Mass Transfer, 26 (2), 289-300.

Allegra JR, Hawley SA (1972). Attenuation of sound in suspensions and emulsions: Theory and experiments, Journal of Acoustical Society of America, 51 (5), 1545-1564.

Bamberger JA, Greenwood MS (2004). Using ultrasonic attenuation to monitor slurry mixing in real time. Ultrasonics, 42, 145-148.

Basaran TK, Demetriades K, McClements DJ (1998). Ultrasonic imaging of gravitational separation in emulsions. Colloids and Surfaces A: Physicochemical and Engineering Aspects, 136, 169-181.

Beckett ST (2001). Milling, mixing and tempering – an engineering view of chocolate. Proceedings of the Institution of Mechanical Engineers, 215 (E), 1-8.

Beckett ST (2009). Conching. In Industrial Chocolate Manufacture and Use. (4th Ed). Edited by Beckett ST, pp. 192-223. John Wiley and Sons, Chichester.

Bilaniuk N, Wong GSK (1993). Speed of sound in pure water as a function of temperature. The Journal of Acoustical Society of America, 93 (3), 1609-1612.

Blitz J (1967). Fundamentals of Acoustics (2nd Ed.). Butterworths, London.

Botsaris GD (1976). Secondary nucleation-a review. In Industrial Crystallization. Edited by Mullin JW, p.3. Plenum Press, New York.

Brandon D, Kaplan WD (2008). Microstructural Characterization of Materials (2nd Ed.). John Wiley and Sons, Chippenham.

Bryant CM, McClements DJ (1999). Ultrasonic spectrometry study of the influence of temperature on whey protein aggregation. Food Hydrocolloids, 13, 439-444.

Buma TJ, Wiegers GA (1967). X-ray powder patterns of lactose and unit cell dimensions of β-lactose. Netherlands Milk and Dairy Journal, 21, 208-213.

Challis RE, Povey MJW, Mather ML, Holmes AK (2005). Ultrasound techniques for characterizing colloidal dispersions. Reports on Progress in Physics, 68, 1541-1637.

Chanamai R, Coupland JN, McClements DJ (1998). Effect of temperature on the ultrasonic properties of oil in water emulsions. Colloids and Surfaces A: Physicochemical and Engineering Aspects, 139, 241-250.

Chanamai R, Herrmann N, McClements DJ (2000). Probing floc structure by ultrasonic spectroscopy, viscometry, and creaming measurements. Langmuir, 16, 5884-5891.

Chevalley J (1999). Chocolate flow properties. In Industrial Chocolate Manufacture and Use (3rd Ed.). Edited by Beckett ST, pp. 182-200. Blackwell Science, Oxford.

Coupland JN (2004). Low intensity ultrasound. Food Research International, 537-543.

Darby R (2001). Chemical Engineering Fluid Mechanics (2nd Ed.). Marcel Dekker Inc., New York.

Epstein PS, Carhart RR (1953). The absorption of sound in suspensions and emulsions. I. Water fog in air. Journal of Acoustical Society of America, 25 (3), 553-565.

Faran JJ (1951). Sound scattering by solid cylinders and spheres. Journal of Acoustical Society of America, 23, 405-418.

Figura LO, Epple M (1995). Anhydrous α-lactose. A study with DSC and TXRD. Journal of Thermal Analysis, 44, 45-53.

Foubert I, Dewettinck K, Vanrolleghem PA (2003). Modelling of the crystallization kinetics of fats. Trends in Food Science and Technology, 14, 79-92.

Ganzle MG, Haase G, Jelen P (2008). Lactose: Crystallization, hydrolysis and value-added derivatives. International Dairy Journal, 18, 685-694.

Garnier S, Petit S, Coquerel (2002). Dehydration mechanism and crystallization behavior of lactose. Journal of Thermal Analysis and Calorimetry, 68, 489-502.

Garside J, 1985. Industrial crystallization from solution. Chemical Engineering Science. 40 (1), 3-26.

Gillies DG, Greenley KR, Sutcliffe LH (2006). ESR/spin probe study of ice cream. Journal of Agricultural and Food Chemistry, 54 (14), 4934-4947.

Gulseren I, Coupland JN (2007). Excess ultrasonic attenuation due to solid-solid and solid-liquid transitions in emulsified octadecane. Crystal Growth & Design, 7 (5), 912-918.

Gulseren I, Coupland JN (2008). Ultrasonic properties of partially frozen sucrose solutions. Journal of Food Engineering, 89, 330-335.

Haase G, Nickerson TA (1966a). Kinetic reactions of alpha and beta lactose. I. Mutarotation. Journal of Dairy Sciences, 49 (2), 127-132.

Haase G, Nickerson TA (1966b). Kinetic reactions of alpha and beta lactose. II. Crystallization. Journal of Dairy Sciences, 49 (7), 757-761.

Haque MDK, Roos YH (2005). Crystallization and X-ray diffraction of crystals formed in water-plasticized amorphous spray-dried and freeze-dried lactose/protein mixtures. Journal of Food Science E: Food Engineering and Physical Properties, 70 (5), E359-E366.

Harker AH, Temple JAG (1988). Velocity and attenuation of ultrasound in suspensions of particles in fluids. Journal of Physics D-Applied Physics, 21 (11), 1576-1588.

Hartel RW (2001). Crystallization in Foods. Aspen Publishers, Inc., Maryland.

Hay A, Mercer D (1985). On the theory of sound scattering and viscous absorption in aqueous suspensions at medium and short wavelengths. Journal of Acoustical Society of America, 78, 1761-1771.

Herrington BL (1934). Some physico-chemical properties of lactose. II. Factors influencing the crystalline habit of lactose. Journal of Dairy Science, 17 (8), 533-542.

Higami M, Ueno S, Segawa T, Iwanami K, Sato K (2003). Simultaneous synchrotron radiation X-ray diffraction - DSC analysis of melting and crystallization behavior of trilauroylglycerol in nanoparticles of oil-in-water emulsion. Journal of the American Oil Chemists Society, 80 (8), 731-739.

Hipp AK, Walker B, Mazzotti M, Morbidelli M (2000). In-situ monitoring of batch crystallization by ultrasound spectroscopy. Industrial and Engineering Chemistry Research, 39, 783-789.

Holmes AK, Challis RE, Wedlock DJ (1993). A wide bandwidth study of ultrasound velocity and attenuation in suspensions: Comparison of theory with experimental measurements. Journal of Colloid and Interface Science, 156, 261-268.

Holmes AK, Challis RE, Wedlock DJ (1994). A wide bandwidth ultrasonic study of suspensions: the variation of velocity and attenuation with particle size. Journal of Colloid and Interface Science, 168, 339-348.

Holmes AK, Challis RE, Chen Y, Hibberd DJ, Moates GK (2007). Ultrasonic scattering in chocolate and model systems containing sucrose, tripalmitin and olive oil. IEEE Transactions on Ultrasonics, Ferroelectrics, and Frequency Control, 54 (11), 2357-2366.

Holsinger VH (1997). Physical and chemical properties of lactose. In Advanced Dairy Chemistry Vol 3. (2nd Ed.). Edited by Fox PF, pp. 1-31. Chapman and Hall, London.

Hudson CS (1908). Further studies on the forms of milk-sugar. Journal of the American Chemical Society, 30 (11), 1767-1783.

Hunziker OF, Nissen BH (1926). Lactose solubility and lactose crystal formation. I. Lactose solubility. Journal of Dairy Sciences, 9 (6), 517-537.

Hunziker OF, Nissen BH (1927). Lactose solubility and lactose crystal formation. II.Lactose crystal formation. Journal of Dairy Sciences, 10 (2), 139-154.

Johansson D, Bergenstahl B (1992a). The influence of food emulsifiers on fat and sugar dispersions in oils. II. Rheology, colloidal forces. Journal of the American Oil Chemists Society, 69 (8), 718-727.

Johansson D, Bergenstahl B (1992b). The influence of food emulsifiers on fat and sugar dispersions in oils. I. Adsorption, Sedimentation. Journal of the American Oil Chemists Society, 69 (8), 705-717.

Johansson D, Bergenstahl B (1992c). The influence of food emulsifiers on fat and sugar dispersions in oils. III. Water content, purity of oils. Journal of the American Oil Chemists Society, 69 (8), 728-733.

Johansson D, Bergenstahl B (1995). Sintering of fat crystal networks in oil during post crystallization processes. Journal of the American Oil Chemists Society, 72, 911-920.

Karpinski PH, Wey JS (2001). Precipitation processes. In Handbook of Industrial Crystallization, 2nd Ed. Edited by Myerson AS, pp.141-160. Butterworth-Heinemann, Boston.

Kasapis S, Al-Marhoobi IM, Deszczynski M, Mitchell JR, Abeysekera R (2003). Gelatin vs polysaccharide in mixture with sugar. Biomacromolecules, 4, 1142-1149.

Kinsler LE, Frey AR, Coppens AB, Sanders JV (2000). Fundamentals of Acoustics (4th Ed.). John Wiley & Sons, Hoboken.

Labuza TP, Labuza PS (2004). Influence of temperature and relative humidity on the physical states of cotton candy. Journal of Food Processing Preservation, 28, 274-287.

Lloyd P, Berry MV (1967). Wave propagation through an assembly of spheres. IV. Relations between different multiple scattering theories. Proceedings of the Physical Society, 91, 678–688.

Marangoni AG (1998). On the use and misuse of the Avrami equation in characterization of the kinetics of fat crystallization. Journal of the American Oil Chemists Society, 75, 1465-1467.

Marshall T, Challis RE, Holmes AK, Tebbutt JS (2002). Modeling ultrasonic compression wave absorption during the seeded crystallization of copper (II) sulphate pentahydrate from aqueous solution. IEEE Transactions on Ultrasonics, Ferroelectrics, and Frequency Control, 49 (11), 1583-1591.

Martini S, Bertoli C, Herrera ML, Neeson I, Marangoni A (2005). Attenuation of ultrasonic waves: influence of microstructure and solid fat content. Journal of the American Oil Chemists Society, 82(5), 319-328.

McClements DJ, Povey MJW (1989). Scattering of ultrasound by emulsion. Journal of Physics D: Applied Physics, 22, 38-47.

McClements DJ, Fairley P (1992). Frequency scanning ultrasonic pulse echo reflectometer. Ultrasonics, 30 (6), 403-405.

McClements DJ, Povey MJW, Dickinson E (1993). Absorption and velocity dispersion due to crystallization and melting of emulsion droplets. Ultrasonics, 31 (6), 433-437.

Mimouni A, Schuck P, Bouhallab S (2005). Kinetics of lactose crystallization and crystal size as monitored by refractometry and laser light scattering: effects of proteins. Lait, 85, 253-260.

Mongia G, Ziegler GR (2000). The role of particle size distribution of suspended solids in defining the flow properties of milk chocolate. International Journal of Food Properties, 3(1), 137-147.

Myerson AS, Ginde R (2001). Crystals, crystal growth, and nucleation. In Handbook of Industrial Crystallization (2nd Ed). Edited by Myerson AS, pp. 33-65. Butterworth-Heinemann, Boston

Nelson RD Jr. (1988). Dispersing powders in liquids. In Handbook of Powder Technology (Vol. 7). Edited by Williams JC and Allen T, pp 245. Elsevier, Amsterdam.

Nickerson TA (1962). Lactose crystallization in ice cream. IV. Factors responsible for reduced incidence of sandiness. Journal of Dairy Science, 45 (3), 354-359.

Nickerson TA and Moore (1974). Factors influencing lactose crystallization. Journal of Dairy Science, 57 (11), 1315-1319.

Omar W, Ulrich J (1999). Application of ultrasonics in the on-line determination of supersaturation. Crystal Research and Technology, 34, 379-389.

Pinfield VJ, Dickinson E, Povey MJW (1994). Modeling of concentration profiles and ultrasonic velocity profiles in a creaming emulsion: Importance of scattering effects. Journal of Colloid and Interface Science, 166, 363-374.

Pinfield VJ, Povey MJW, Dickinson E (1995). The application of modified forms of the Urick equation to the interpretation of ultrasound velocity in scattering systems. Ultrasonics, 33 (3), 243-251.

Povey MJW (1997). Ultrasonic Techniques for Fluid Characterization. Academic Press, San Diego, California.

Raghavan SL, Ristic RI, Sheen DB, Sherwood JN (2001). The bulk crystallization of α-lactose monohydrate from aqueous solution. Journal of Pharmaceutical Sciences, 90 (7), 823-832.

Raghavan SL, Ristic RI, Sheen DB, & Sherwood JN (2002). Dissolution kinetics of single crystals of α-lactose monohydrate. Journal of Pharmaceutical Sciences, 91 (10), 2166-2174.

Richter A, Babick F, Ripperger S. (2005). Polydisperse particle size characterization by ultrasonic attenuation spectroscopy for systems of diverse acoustic contrast in the large particle limit. Journal of Acoustical Society of America, 118 (3), 1394-1405

Richter A, Babick F, Stintz M (2006). Polydisperse particle size characterization by ultrasonic attenuation spectroscopy in the micrometer range. Ultrasonics, 44, e483-e490.

Saggin R, Coupland JN (2002). Ultrasonic monitoring of power dissolution. Journal of Food Science, 67 (4), 1473-1477.

Saggin RS, Coupland JN (2004). Shear and longitudinal ultrasonic measurements of solid fat dispersions. Journal of the American Oil Chemists Society, 81, 27-32.

Sayan P, Ulrich J (2002). The effect of particle size and suspension density on the measurement of ultrasonic velocity in aqueous solutions. Chemical Engineering and Processing, 41, 281-287.

Singh AP, McClements DJ, Marangoni AG (2002). Comparison of ultrasonic and pulsed NMR techniques for determination of soldi fat content. Journal of the American Oil Chemists Society, 79 (5), 431-437.

Tebbutt JS, Challis RE (1996). Ultrasonic wave propagation in colloidal suspensions and emulsions: a comparison of four models. Ultrasonics, 34, 363-368.

Tebbutt JS, Marshall T, Challis RE (1999). Monitoring of copper (II) sulfate pentahydrate crystallization using ultrasound. Langmuir, 15, 3356-3364.

Titiz-Sargut S, Ulrich J (2003). Application of a protected ultrasound sensor for determination of the width of the metastable zone. Chemical Engineering and Processing, 42, 841-846.

Twieg WC, Nickerson TA (1968). Kinetics of lactose crystallization. Journal of Dairy Science, 51 (11), 1720-1724.

Ulrich J, Strege C (2002). Some aspects of the importance of metastable zone width and nucleation in industrial crystallizers. Journal of Crystal Growth, 237-239, 2130-2135.

Ulrich J (2003). Solution crystallization – developments and new trends. Chemical Engineering and Technology, 26, 832-835.

Walstra P, Jenness R (1984). Dairy Chemistry and Physics. John Wiley & Sons, New York.

Waternan PC, Truell R (1961). Multiple scattering of waves. Journal of Mathematical Physics, 4 (2), 512-537.

Whitaker R (1933). Some factors influencing the crystallization of lactose in ice cream. Journal of Dairy Science, 16 (3), 177-202.

Whittier EO (1944). Lactose and its utilization: A Review. Journal of Dairy Science, 27 (7), 505-537.

Wright AJ, Narine SS, Marangoni AG (2000). Comparison of experimental techniques used in lipid crystallization studies. Journal of the American Oil Chemists Society, 77, 1239-1242.

Ziegler GR, Benado AL, Rizvi SH (1987). Determination of mass diffusivity of simple sugars in water by the rotating disk method. Journal of Food Science, 52 (2), 501-502.

Appendix A

Supplementary Material for Chapter 3

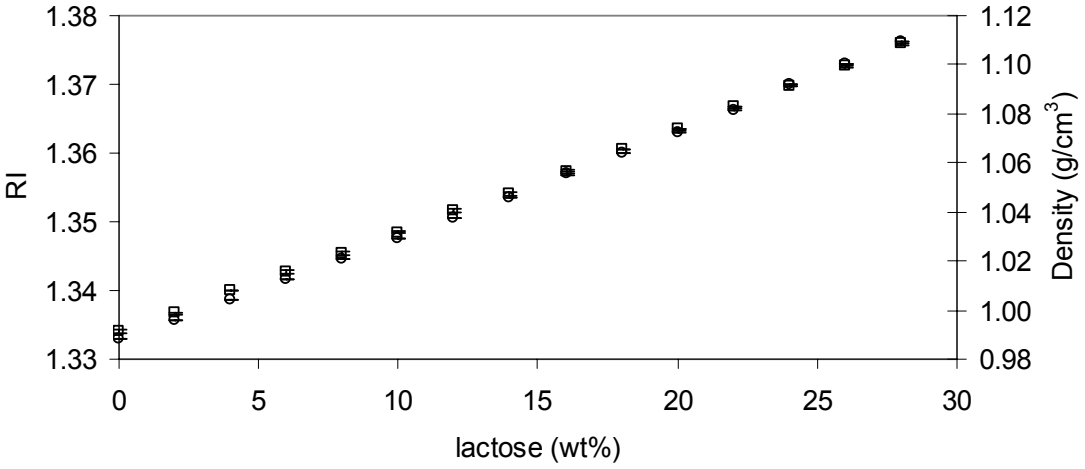

Figure A.1. Density (□) and refractive index (○) calibrations for lactose solutions. Points and error bars are the mean and standard deviation of three experimental replications, respectively.

Appendix B

Supplementary Material for Chapter 4

Figure B.1. Photograph of lactose crystallized from 43 wt% lactose and (left) 1.5 and (right) 3 wt% gelatin solutions after 4-5 hours crystallization started.

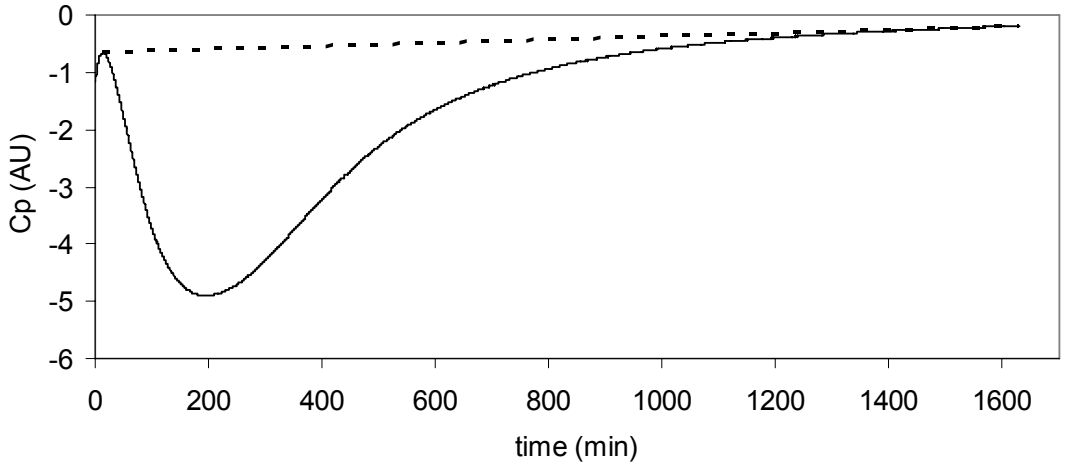

Figure B.2. DSC thermogram of 1.5% gelatin-43% lactose at 25°C and corresponding base-line construction.

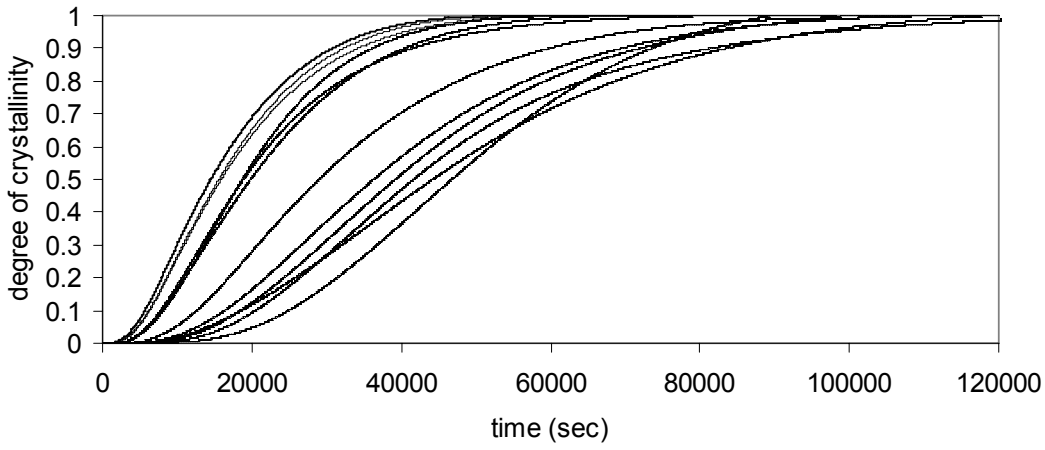

Figure B.3. Lactose crystallization as calculated from isothermal DSC at 25°C for aqueous solutions of (···) 1.5 wt% gelatin and 43 wt% lactose, (− −) 3 wt% gelatin and 43 wt% lactose. (—) 1.5 wt% gelatin and 46 wt% lactose, (-·-) 3 wt% gelatin and 46 wt% lactose. All 3 replications for each treatment were shown on the graph.

Appendix C

Supplementary Material for Chapter 5

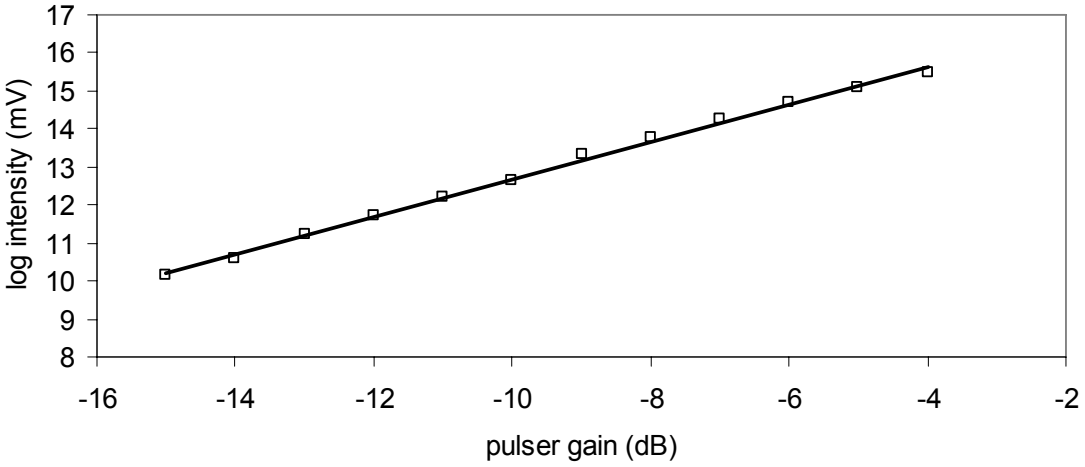

Figure C.1. Change in acoustic intensity with pulser gain in water as used for calibration. The linear regression line ($y = 0.493x + 17.618$, $R^2 = 0.999$) was shown on the graph.

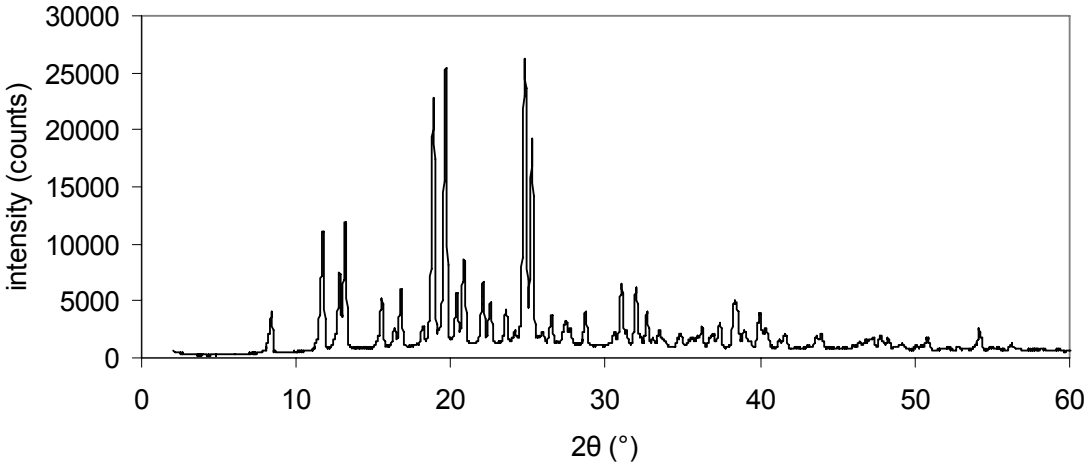

Figure C.2. XRD pattern of the confectioner's sugar sample used.

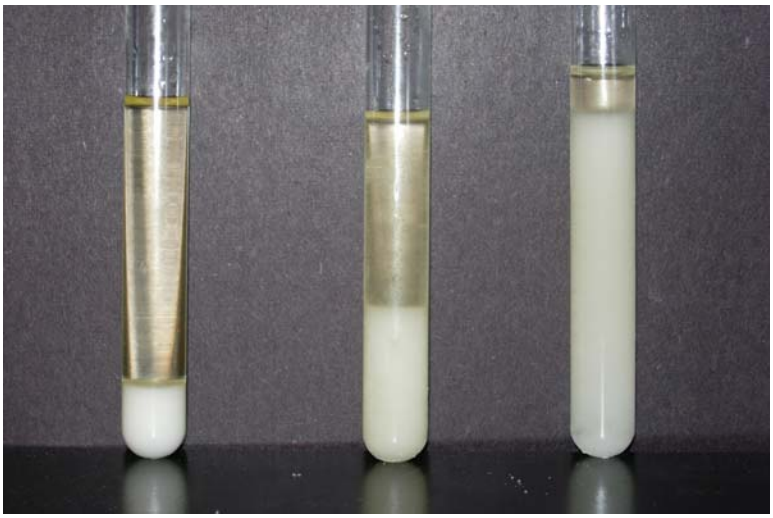

Figure C.3. Picture showing the effect water addition to 8 wt% sucrose in corn oil dispersions. From left to right: 0, 0.5, and 1% (vol water/wt lactose).